EXPERIMENTAL INVESTIGATION OF PERFORATED CONICAL SHELLS

A Thesis Submitted
in Partial Fulfilment of the Requirements
for the Degree of
MASTER OF TECHNOLOGY

by
SIDDH NATH GUPTA

to the

DEPARTMENT OF AEROSPACE ENGINEERING
INDIAN INSTITUTE OF TECHNOLOGY KANPUR
MAY, 1991

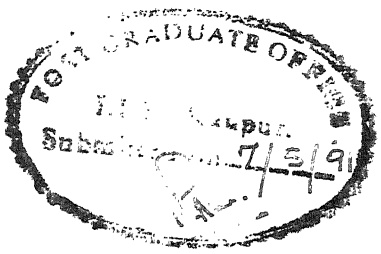

CERTIFICATE

This is to certify that the thesis entitled, "**Experimental Investigation of Perforated Conical Shells** " , is a record of the work carried out under my supervision by Mr. Siddh Nath Gupta and that it has not been submitted elsewhere for awarding a degree .

A. K. Gupta

Dated : 7-5-91 (Dr . A . K Gupta)

Professor and Head of the department

Department of Aerospace Engineering

Indian Institute of Technology

KANPUR

ACKNOWLEDGEMENTS

I am immensely indebted to Dr. A . K . Gupta for his perserving and seminal guidance through out the course of this work .

Thanks are due to Mr. H. C. Bhattacharya and his team of dedicated workers for a nice job done in fabricating the models .

I am also grateful to Shri . K . S . Muddappa for his constant help throughout the course of this work .

I am also thankful to Mr . C . V . K . Singh for his constant encouragement . Thanks are also due to Mr. Rajeeva Kumar and Mr. Sujoy Datta for the same .

(Siddh Nath Gupta)

CONTENTS

ABSTRACT

The purpose of this study was to obtain data on the aerodynamic forces on perforated conical shells . The force tests on perforated conical shells were performed in a wind tunnel . Two parameters have been varied in the measurement of the data for the perforated conical shells . One was the included cone angle and the other was the wire mesh size (i.e. the amount of perforation) of the conical shell . Four included cone angles namely — 30°,60°,90°,180° have been used for the perforated conical shells , each of which was made up of four different types of wire meshes . These models were mounted in the wind tunnel test section and forces were measured using a 3—component aerodynamic balance with wind speeds varying from 15 to 27 m/s . The Reynolds number during the present study was kept in the range of 1.6×10^5 to 3.0×10^5 .

Similiar aerodynamic tests on cones having included angles 30°, 60°, 90°, 180° were also carried out , in order to compare the results with the already

known results , for solid cones.

The variation of drag and side force [lift] of the models with the wind speed is presented . It has been observed that there is some asymmmetry in the flow around the perforated cone . This is due to the fact that the fabricated conical shells made of wire mesh were not perfect in shape and there was a certain lack of symmetry in their shape.

Even in the face of such drawbacks the measured drag coefficients for various solid cones compare well with the earlier studies and give a fair idea of the forces acting on the perforated conical shells of different mesh sizes and included angles .

LIST OF SYMBOLS

C_D	Drag coefficient
C_L	Lift coefficient
D	Drag
d	Diameter of the conical shell
L	Lift
Re	Reynolds Number
S	Surface area
V	Wind speed
ρ	Density of the air

LIST OF PHOTOGRAPHS

LIST OF FIGURES

CHAPTER 1

INTRODUCTION

Ingestion of birds into the turbojet engines during take—off and landing phases of flights , have been a serious concern to the designers of aircraft engines . There have been considerable loss of life and damage to material due to accidents arising from bird hits .

Recently Dr. A.K.Gupta, in an unpublished abstract [see : Appendix 1] has proposed the installation of a perforated conical shell shroud ahead of the turbojet intake [of the aircraft engine] at the time of take—off and landing to prevent bird ingestion in to the engines . The proposed bird—hit prevention device shall be operable up to a height of one kilometer above ground after which it shall be retracted into the engine nacelle .

This perforated conical shell shall , probably be made from wire mesh , the amount of perforation

depending on the size of the debris to be prevented from being ingested into the engine . Another important factor that will have to be taken into account is the amount of air flow that will be obstructed due to the installation of such a device in front of the engine intake .

Apart from the above considerations , there are two other major aspects to the proposed bird ingestion prevention device :—

[a] Aerodynamic aspect : This basically deals with the aerodynamic forces that will be generated due to the installation of the perforated conical shell, the most important of them being 'Drag' . To make the device viable it will be necessary to check the amount of drag generated .

The present work has dealt with the aerodynamic aspect of the problem . The idea was to measure the variation of the drag coefficient with the change in the parameters of the perforated conical shells . The parameters that have been varied in the present work are the amount of perforation and the included cone angle . The tests were conducted in the wind tunnel on

different models .

[b] Structural Aspects : This aspect deals with the structural strength requirements of the perforated conical shell in order to withstand the aerodynamic forces and the impact forces of the debris on the conical shell .

A large volume of data was available regarding the drag coefficients etc. for solid cones but none could be found for perforated cones . The other compelling motivation behind the study was purely academic , as there was no data available regarding the aerodynamics of perforated conical shells . This study investigated the variation of the drag coefficient of the perforated conical shell with the wire mesh size and the included cone angle of the perforated conical shell .

CHAPTER 2

EXPERIMENTAL EQUIPMENT

2.1 THE WIND TUNNEL AND ITS SPECIFICATIONS

The subsonic wind tunnel (known as the 5-D tunnel) at the low speed aerodynamics laboratory of I.I.T Kanpur was used . The tests were conducted in the 3-D test section . It is a closed circuit type wind tunnel , having a rectangular cross section of 915 mm X 610 mm with a length of 1675 mm . The characterstics of the motor are as follows :—

	SCR	DC	BLOWER DRIVE
	Twin		15 HP
Input	400 V	50 cycles 3 phase	
	57-98-57 Amperes		
Output	Armature	115 V	110 Amperes DC
	Field	115 V	5-7 Amperes DC

The motors were turned on by pressing the start buttons of the respective units and their speeds were then controlled by the manual speed adjusting

potentiometers · The maximum velocity obtainable was 42 m/s · Wind speed was measured by using a pitot static tube in the test section ·

2·2 WIND SPEED MEASUREMENT

For measuring the wind speed the Furness type digital micro-manometer was used · The static and stagnation tubes of the pitot static tube were connected to it · This device , then , displayed the velocity as well as the inches of water digitally · The maximum pressure difference that could be measured by this micro-manometer was 19.99 inches of water ·

2·3 3- COMPONENT BALANCE

The balance had two frames — one , with which it was attatched to the supporting base and the other , which was movable and transfered the load to the load cells ·

The load cells consisted of high precision strain

gauges with excellent repeatability and linearity characterstics which measured the load displayed on the digital panels .

The geometrical construction of the load sensing system allowed the complete seperation and independent measurement of Lift , Drag and Pitch with negligible interactions between them .

The maximum load that the balance can measure is as follows :

LIFT - 120 Newton

DRAG - 60 Newton

PITCH MOMENT - 2.5 N-m

CHAPTER 3

EXPERIMENTAL TECHNIQUE AND MODEL MOUNTING

3·1 STATIC CALIBRATION OF THE BALANCE

3·1·1 LIFT CALIBRATION

This was the simplest of the check calibrations and required that no struts were fitted to the balance and that 1 Kg (9·81 N) brass weights were added directly to the strut platform ·

The balance was unclamped and by adjusting the rectangular tare weights the lift displayed was brought to read zero · Pitch and Drag too were brought to zero at the same time ·

One Kg brass weights were now added to the centre of the strut platform one at a time from 1 to a maximum of 12 Kg · At each step the displayed reading was noted · (Acceleration due to gravity was assumed to be 9·81 (m/s^2))·

Any reading other than zero , present at the

bigining of the test before any load had been applied was subtracted from the displayed reading to obtain the actual load .

3.1.2 DRAG CALIBRATION

The three struts and the calibration model were mounted . Drag calibration pulley was positioned approximately 1 m from the centre of the balance , downstream of the main struts . The groove in the pulley were set to parallel to the balance axis and at the same height as the central hole . Calibration wire was then attatched to the model , passed over the pulley and then the weight hanger was suspended on the other end . Now the balance was unlocked and the tare weight system adjusted to give zero a reading on all displays .

The weight hanger was now loaded , 1 Kg at a time to a maximum of 7 Kg and the standard drag readings were noted .

3·2 MODEL FABRICATION

The model which was mounted in the wind tunnel to measure the aerodynamic forces of a perforated conical shell had two components · One was the perforated conical shell and the other was the frame ·

Each perforated conical shell was made from a wire mesh · Four different kinds of wire meshes were used to give four different conical shells at the same included angle of the perforated conical shell · The specifications and nomenclatures of the wire meshes were as follows :

Type of Wire Mesh	Dia· of Wire X Holes per sq· in·	Remarks
1	0·21 mm X 841	Least perforated
2	0·30 mm X 361	Small perforation
3	0·42 mm X 144	Med· perforation
4	0·75 mm X 25	Large perforation

Apart from the mesh size , the included angle of

the perforated conical shell was also varied . Four different angles have been used . These are 30 , 60 , 90 and 180 degrees . Thus there were sixteen perforated conical shells in total . For all the conical shells the base diameter was kept constant at 160 mm .

To fabricate the perforated conical shells of a constant included angle , a dummy cone of wood was first fabricated , as a template , which had the same included angle as that of the desired perforated conical shell but it was kept 12 mm longer than the desired perforated conical shell to accomodate the frame .

The wire mesh was wrapped around the dummy wooden cone and was cut so that the wire mesh just covered the surface of the dummy cone . Then , the cut wire mesh sheet was stitched with a wire along the slant line of the perforated conical shell . The above process was repeated for each wire mesh thus giving four different perforated conical shells of constant included angle .

Now another dummy cone of a different included angle was fabricated , and then perforated conical shells of the corresponding included angle were fabricated with the help of this new dummy cone . Similarly perforated conical shells of other included angles were also fabricated .

The lengths of the dummy cones and those of their respective perforated conical shells were as follows :

Length of the dummy cone = 12 mm + Length of the desired perforated conical shell

Included angle	Length of true perforated shell	Length of the dummy cone
30°	29·86 cm	31·06 cm
60°	13·85 cm	15·05 cm
90°	8·00 cm	9·20 cm

Frames were used for mounting the perforated conical shells in the wind tunnel . The frames held the conical shells at their base and as the base diameter for each perforated conical shell was a

constant , the frames for different perforated conical shells were identical to each other in every respect .

The frame consisted of three parts (see Fig :19). The first part was a circular strip made of Aluminum , having a width of 12 mm and a diameter of 160 mm (see Fig : 19 [C]) . The second and third parts were identical semi—circular Aluminum strips of diameter 163 mm each , which extended radially outwards from the center , to a length of 115 mm on both the sides (see Fig : 19 [A] and [B]) .

During assembly , the circular aluminum strip was placed inside the base of the perforated conical shell so that the extra 12 mm of the perforated conical shell mesh was covered by the circular strip . The extra 12 mm mesh was bent along the length of the conical shell . Thus :

Length of the model = Length of true perforated conical shell + Length of the frame

Where ,

Length of the frame = width of the Al strip = 12 mm .

Now , the two semi circular aluminum strips were

placed opposite to each other outside the circular strip . The above combination was rivetted along the circumference and in the extended portion of the semicircular strips at several points .

Apart from studying the aerodynamic forces on the perforated conical shells , those on the solid cones were also studied , so as to compare the results with those of the perforated conical shells and to check the validity of the experimental set up by comparing the measured results for the solid cone with those already available in the literature[1,3] . The included angles for the solid cones were kept same as those for the perforated conical shells namely 30° , 60° , 90° and 180° respectively . The solid cones were not made separately , instead the existing perforated conical shells were converted into the corresponding solid cones by wrapping a thick card—board around the wire mesh of the perforated conical shells . The card—board piece was chosen so that it assumed the shape of the perforated conical shells on being wrapped around it . Cellophane tape was used to fix the slant line of the cones . Thick card board bases were added for the base

of the solid conical shells and were fixed using cellophane tape .

3.3 MODEL MOUNTING

The model was mounted in the wind tunnel on the two struts of the 3—component aerodyanamic balance . The third strut of the balance was removed as it was needed only for pitch measurement and the pitch was not of interest in the present study .

To mount the model in the wind tunnel , holes of 8 mm diameter were drilled on each side of the extended portion of the semi—circular strips , equidistant from the centre of the circular strip . The centre to centre distance between the holes was kept at 26 cm (see Fig 19) .

The bolts of each strut were inserted through the holes of the extended portion of the semi circular strips and were tightened using the nuts .

Care was taken to insure that the interaction of the flow around the struts of the aerodynamic balance

and that around the model was a minimum by providing sufficient distance between them . Also to minimise the boundary layer effect , the model was mounted at a height from the floor of the wind tunnel .

3.4 UNCERTANITY IN DATA

Static calibration was done to determine the reliability of the data . It was found that the maximum deviation from the standard value was approximately ± 1.5 % . When the experiments conducted in the wind tunnel were repeated it was found that the maximum deviation was ± 2 % . Repeat tests were conducted on the perforated conical shells of each included angle for wire mesh of type 3 only .

CHAPTER 4

RESULTS AND DISCUSSION

4.1 DATA REDUCTION

True drag of the perforated conical shell was found as follows:

$$\left.\begin{array}{l}\text{True drag of the}\\ \text{perforated conical}\\ \text{shell (D)}\end{array}\right] = \begin{array}{l}\text{drag of the model} -\\ \text{drag of the frame and struts}\end{array}$$

The drag coefficient was calculated as follows

$$C_D = \frac{D}{\frac{1}{2}\rho V^2 S}$$

where $S = \frac{\Pi d^2}{4}$

ρ : density of air

V : wind speed

S : reference area

d : diameter of the perforated shell

Similarly the lift coefficient was calculated as follows

$$C_L = \frac{L}{\frac{1}{2} \rho V^2 S}$$

L : measured lift as given by the 3-component aerodynamic balance

4.2 CALIBRATION RESULTS

Results of the calibration showed that there was a difference in the actual value and the value being shown by the digital display for drag and lift forces both . However , the difference was small and since the response of the balance to both the lift and the drag was still linear , correct readings were got by extrapolation from the values being shown by the digital display . The resultant curves are shown in Figures : 16 and 17 .

4·3 FORCES ON THE MODELS

The forces on the perforated conical shells were studied at four wind speeds namely , 15 m/s, 19 m/s, 23 m/s and 27 m/s · The drag and the lift coefficents, calculated as above were plotted ·

In the subsonic flow , the profile drag consists of the skin friction drag and the pressure drag · Skin friction drag depends upon the surface of the model and is larger for rougher surfaces · The skin friction drag also depends on the contact surface area of the model with the flow · It is larger for bigger contact surfaces · The pressure drag on the other hand depends on the seperation of flow caused by the model · It is larger for blunt surfaces as it causes larger separation ·

Perforated conical shells also generate these two drags · When the perforated conical shell acts like a solid tapered body , the contribution of the pressure drag is less and the predominant factor is the skin friction drag · If the perforated conical shell acts

like a solid blunt body the contribution due to the pressure drag is more and it forms a larg part of the total drag .

When the perforated conical shells can not behave like a solid body and act like a true perforated body, the pressure drag is much smaller than the skin friction drag as there is no flow separation and the air passes through the perforations of the perforated conical shells . In this case the total drag , comprising largely of skin friction drag , is more for surfaces having larger contact area with the flow .

The actual perforated conical shell lies in between the two extreme cases of behaviours outlined above . It behaves more like a solid cone when the perforation of the wire mesh used in the fabrication of perforated conical shell is too small . On the other hand , it behaves more like a perforated model when the perforation of the wire mesh is large . These results can be interpreted from the figures plotted .

In Fig : 5 , the drag coefficients have been plotted as a function of the velocity , for the mesh of Type 1 . The parameter being varied is the included

cone angle of the perforated conical shell . As mentioned earlier , the mesh of Type 1 has the least perforation i.e. it behaves like a solid sheet and hence the perforated conical shell behaves like a solid conical shell . This can be observed by studying Fig : 5 which shows that the drag of the perforated conical shell is the largest for the included angle 180° (flat) and the least for the included angle 30° . Drag for the included angle 90° is greater than that for the included angle 60° which in turn is greater than the drag for the included angle 30° . A similar pattern would have been observed for the solid conical shell . Therefore perforated conical shells of wire mess 1 behave like solid cones .

Drag coefficients for the mesh of Type 2 have been plotted in Fig : 6 . The mesh of type 2 is more perforated than the mesh of Type 1 . Its perforation is large enough for it to behave more like a truly perforated conical shell . This is confirmed by the figure which shows that the drag for the conical shell with included angle 30° is the highest followed by the included angles 60° and 90° . There is a irregularity

as the drag of 180° is not the lowest as it should be for the true perforated case because its contact area with the flow is the least . This can be explained by incorporating the pressure drag that would have come into the picture for the included angle of 180° since the wire mesh used is not as much perforated as to allow it to behave as a true perforated conical shell.

For the mesh of Type 3 (Fig : 7) , the pattern is similar to the mesh of Type 2 except that the drag for the 180° conical shell is lesser than that for the 30° and 60° conical shell (in mesh of Type 2 it was lower than that for the 30° conical shell but greater than that for the 60° conical shell) . This can be explained by the fact that perforation of mesh 3 is greater than that of mesh 2 . This will cause more air to pass through the holes of the perforated sheet rather than being obstructed by it and hence the separation of the flow will be lesser resulting in a smaller pressure drag . In a similar way the figure for mesh of Type 4 can be explained .

If the perforated conical shell is placed in front of the aircraft engine the perforation of the

wire mesh should be minimised to avoid even the tiny debris from getting into the engine . In this case , the perforated conical shell will start acting like a solid conical shell and hence , to minimise the drag the included angle should be less . This will lead to a larger length of the perforated conical shell and hence create structural problems like flutter etc. On the other hand if the perforation is too high the drag of the perforated conical shell will decrease with increase in the included angle . Then the length of the perforated conical shell will be smaller , but the size of the debris entering the engine will be larger. So a compromise has to be made in the size of the wire mesh with regard to the structural problem .

Apart from plotting the drag coefficients versus velocity for a wire mesh cone , the drag coefficients for a particular included angle treating mesh size as a parameter have also been plotted (Figures : 1, 2, 3 & 4) . The results were as expected and the drag for a particular included angle increased from the wire mesh of type 4 to the wire mesh of type 1 .

To check the validity of the experimental set up

the drag for solid cones of included angle 30°, 60°, 90° & 180° was found · Drag coefficients for these solid cones have been plotted in Fig : 9 · Obtained drag coefficients of solid cones have been compared with the known standard values[1,3] in Fig :10, Fig :11, Fig :12 , Fig :13 · Errors in the experimental results for the solid cones have been calculated to be approximately 9.1 % , 10.0 % , 13.2 % & 20.0 % for the included angles 30° , 60° , 90° & 180° respectively · Error in the flat solid disc (180°) was found to be too high · This error had arisen because , as mentioned earlier , no separate solid cones were fabricated rather the perforated conical shells were converted to the corresponding solid cones and the solid cone thus made was not a true one because of the frame · Other possible sources of error could be due to the interaction of the flow around the struts with that around the model ·

Apart from plotting the drag coefficient of the perforated conical shells , the lift coefficients have been plotted for two cases only (Figures : 14 & 15) · As the model is a conical shell , and hence

symmetric , it should not have any lift coefficient , but it turned out to have some non—zero lift ; though very small when compared with the drag · This showed that the models fabricated were not perfectly synmmetric · This can be seen in the photographs of the model · This assymetry is highest for the models of included angle 30° (i·e· the longest ones) and for the models made up of wire mesh of type 1 which had the highest resilience · It was tried to keep this fabrication error a minimum but it could not be removed fully ·

CHAPTER 5

CONCLUSIONS AND SUGGESTIONS FOR FURTHER WORK

Wind tunnel tests on perforated conical shells of various mesh sizes and included cone angles were carried out to find the drag and the lift coefficients at various speeds . Also , the drag coefficients of solid cones of different cone angles were found in order to check the validity of the experimental set up. Different figures of the drag coefficient show that for low perforated conical shells , the drag coefficient varies more or less as that for the solid cones . For highly perforated conical shells , the contribution of the pressure drag in the total drag is comparatively smaller than that for the dense perforated conical shells . For a particular cone angle , the drag coefficient is more for a densely perforated conical shells when compared to the less perforated ones . Non—zero lift coefficients of perforated conical shells show that there was some fabrication error and that they were not symmetric .

Drag coefficients of solid cones were found to be matching well with the standard results except for the solid disc .

The present work is a simplified approach to what is otherwise a very complex problem . Only the drag and side force component were measured at an angle of attack zero . The angle of attack of the wind can be varied to study the yaw effect of the model . In that case the pitching moment will also come into the picture .

If the perforated conical shell is mounted at the intake of an aircraft engine , an important parameter is the mass flow rate through the perforated conical shell . If the wiremesh is too dense the mass flow rate through the conical shell will be less , affecting adversely the performance of the engine . So the variation of the mass flow rate with the amount of perforation could be studied in the wind tunnel as an important parameter .

It will also be of interest to observe the flow around such models using flow visualisation techniques

like smoke tunnels to get a better physical picture of this phenomenon .

In the present work , a frame has been used to hold the perforated conical shell in the wind tunnel . Since the frame consists of metal strips , it produces a drag of about 20 % of the drag of the perforated conical shell . Though the drag due to the frame and the struts has been deducted from the total drag , it could be the cause of errors in the true drag due to the interaction between the flows around the perforated conical shells and the frame . To minimise the auxillary drag , the model should be mounted in the wind tunnel using minimum accessories . One technique could be the use of metal wires to hold the perforated conical shell in the wind tunnel . Other mounting techniques could also be used to mount the perforated conical shell to give better results .

REFERENCES

1. Hoerner, S.F., Fluid Dynamics Drag, Author New Jersey (1965).

2. Pankhurst, R. C., Wind Tunnel Techniques.

3. Blevin , Robert D . , Applied Fluid Dynamics Handbook , Van Nostrand Reinhold Co (1984) .

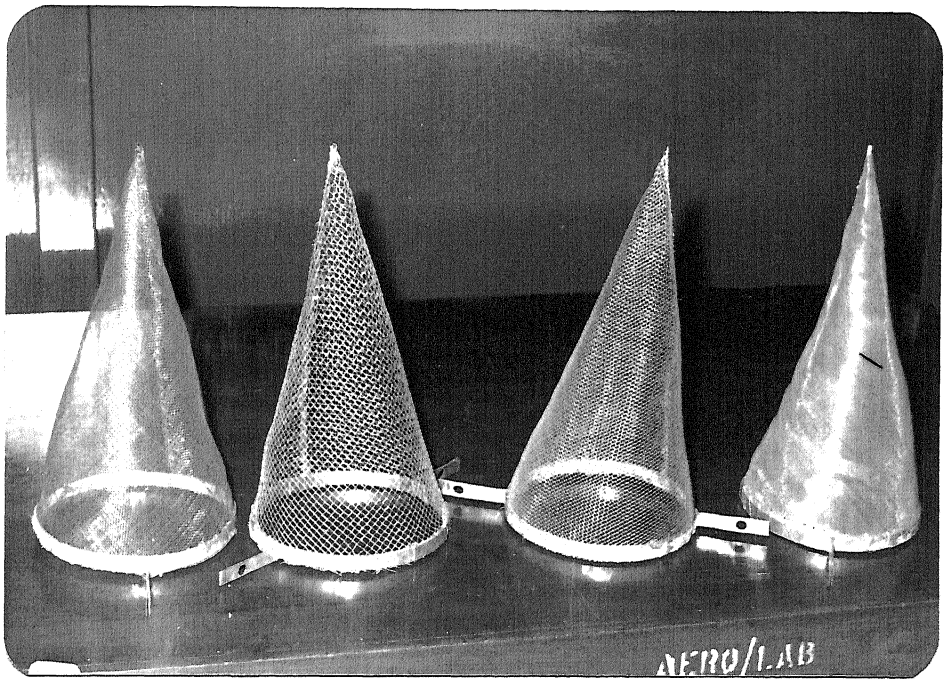

Photo 1 : Perforated Conical shells of included angle 30 deg

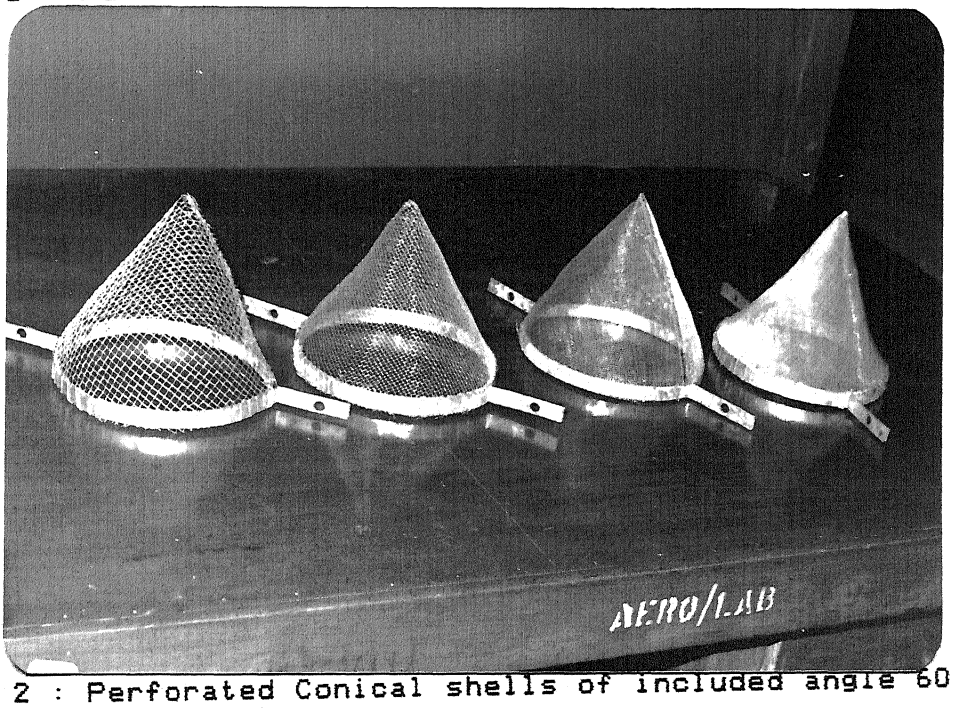

Photo 2 : Perforated Conical shells of included angle 60 deg

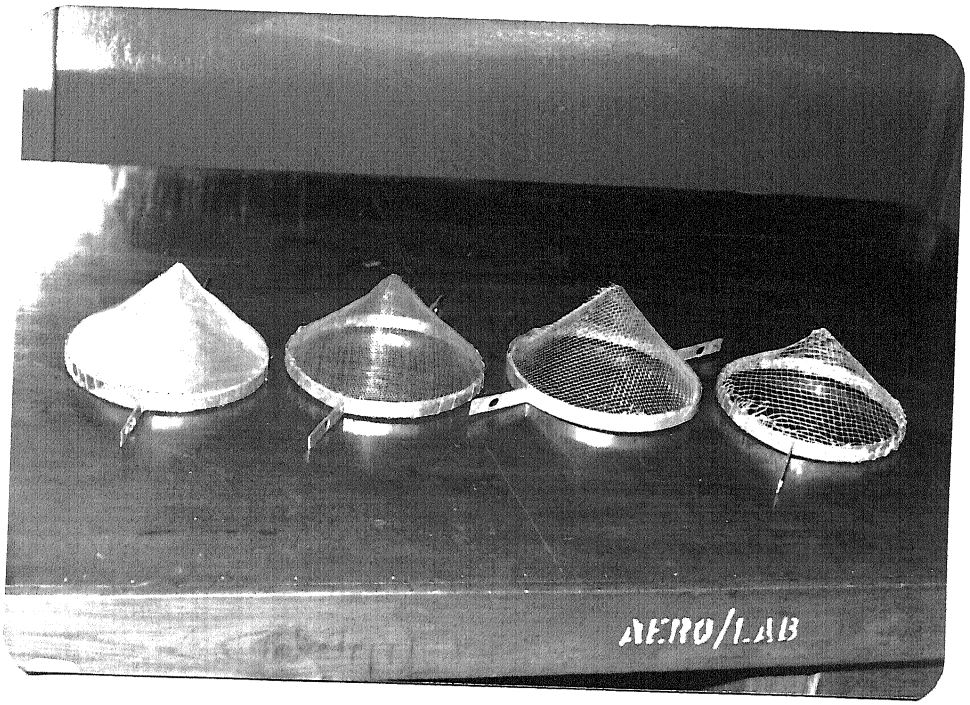

Photo 3 : Perforated Conical shells of included angle 90 deg

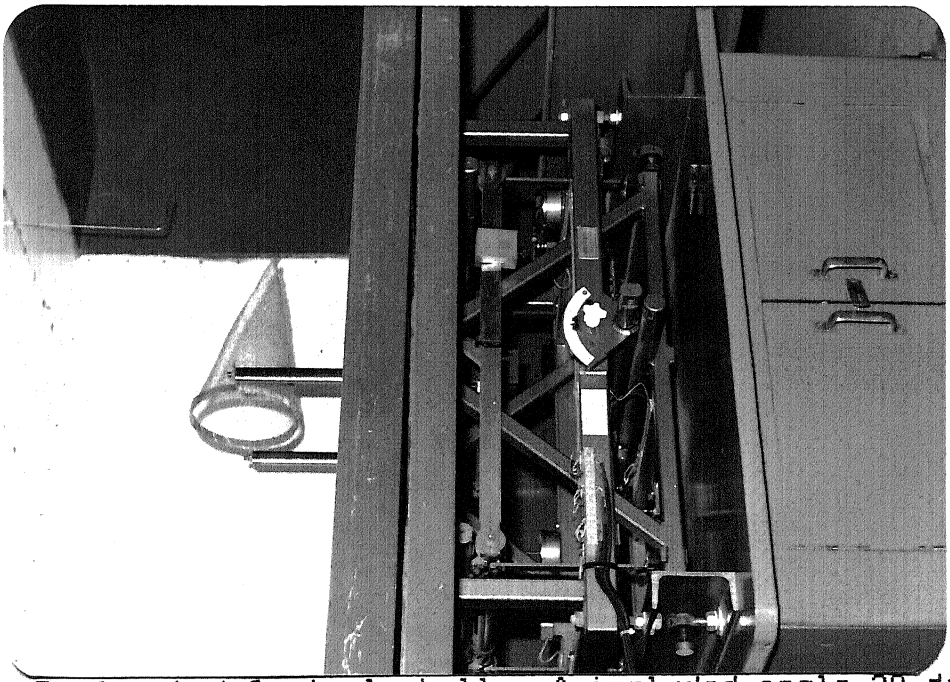

Photo 4 : Perforated Conical shells of included angle 30 deg as mounted

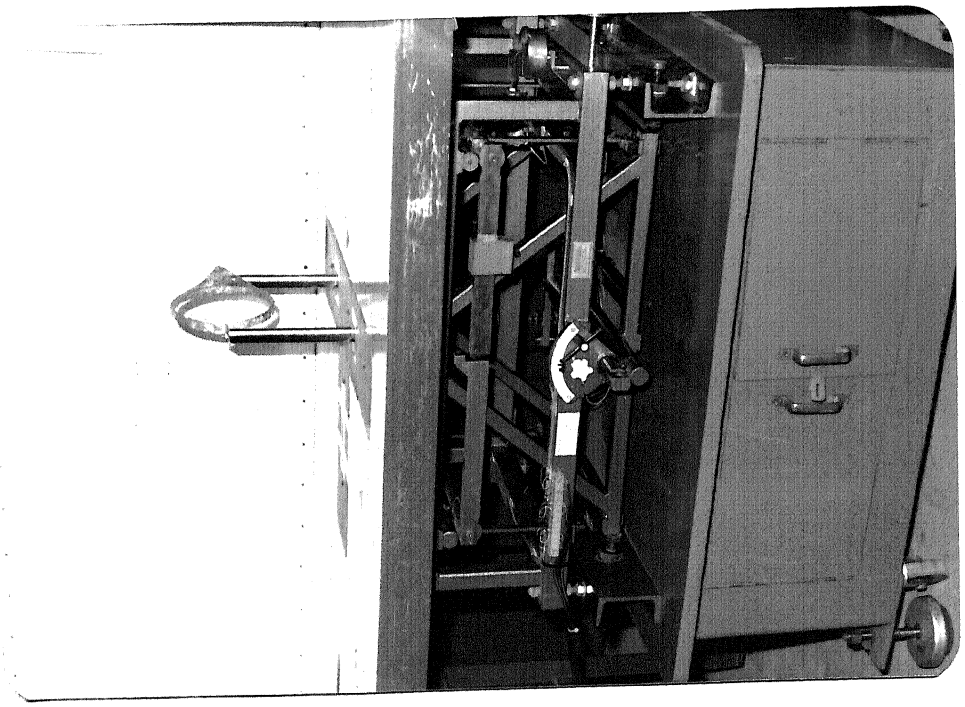

Photo 5 : Perforated Conical shells of included angle 90 deg as mounted

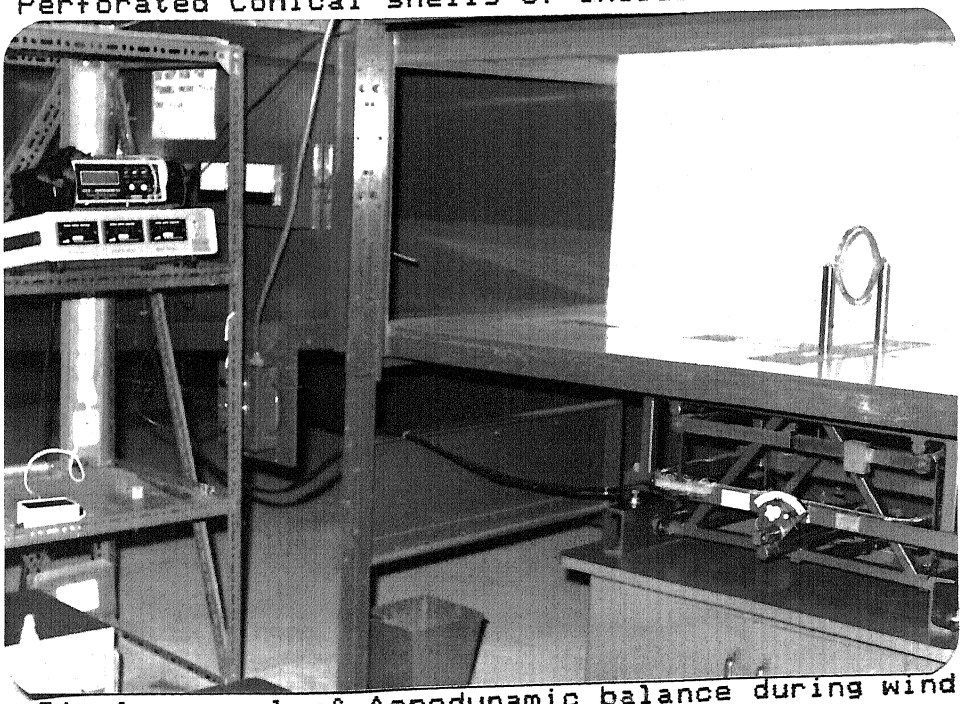

Photo 6 : Display panel of Aerodynamic balance during wind tunnel test

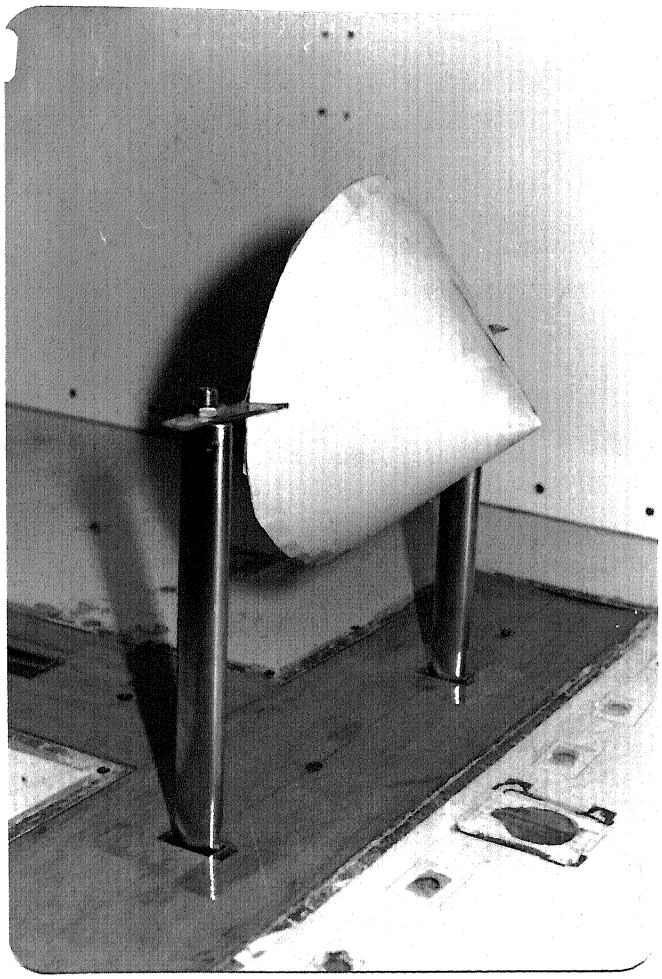

Photo 7 : Solid Cone of included angle 90 deg as mounted in wind tunnel

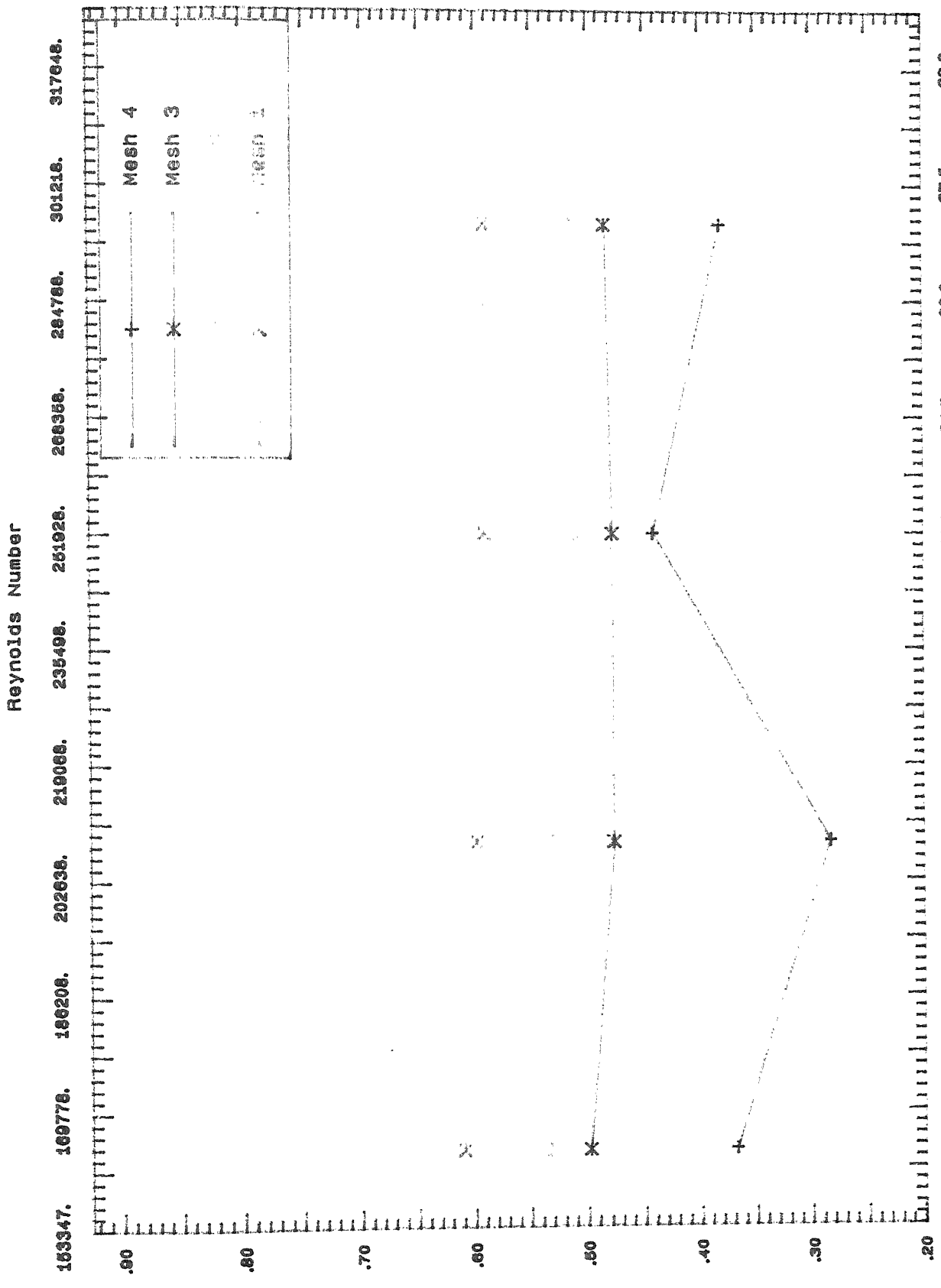

Fig 1 : Drag Coeff. for Included Cone Angle = 30 deg.

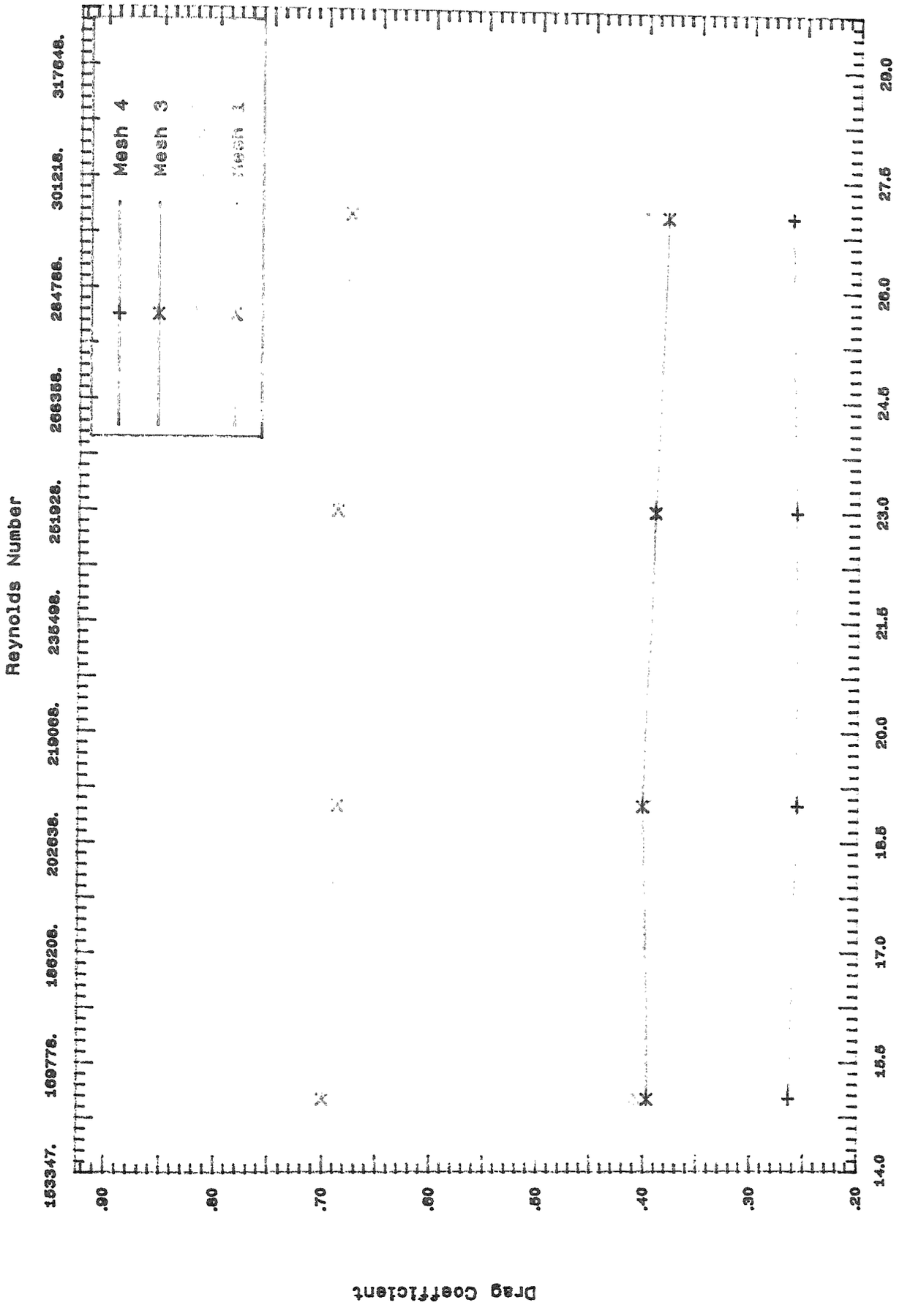

Fig 2 : Drag Coeff. for Included Cone Angle = 60 deg.

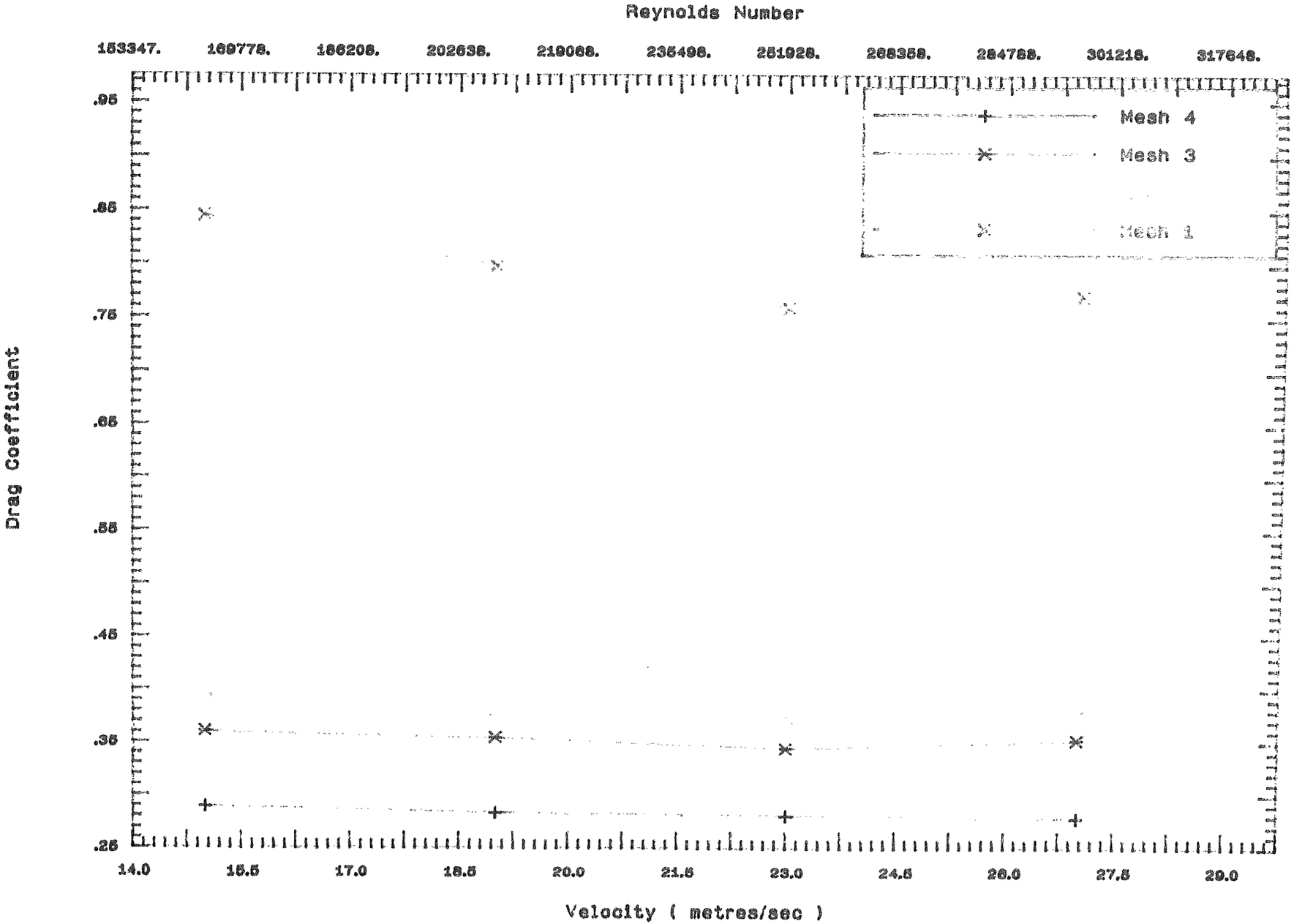

Fig 3 : Drag Coeff. for Included Cone Angle = 90 deg.

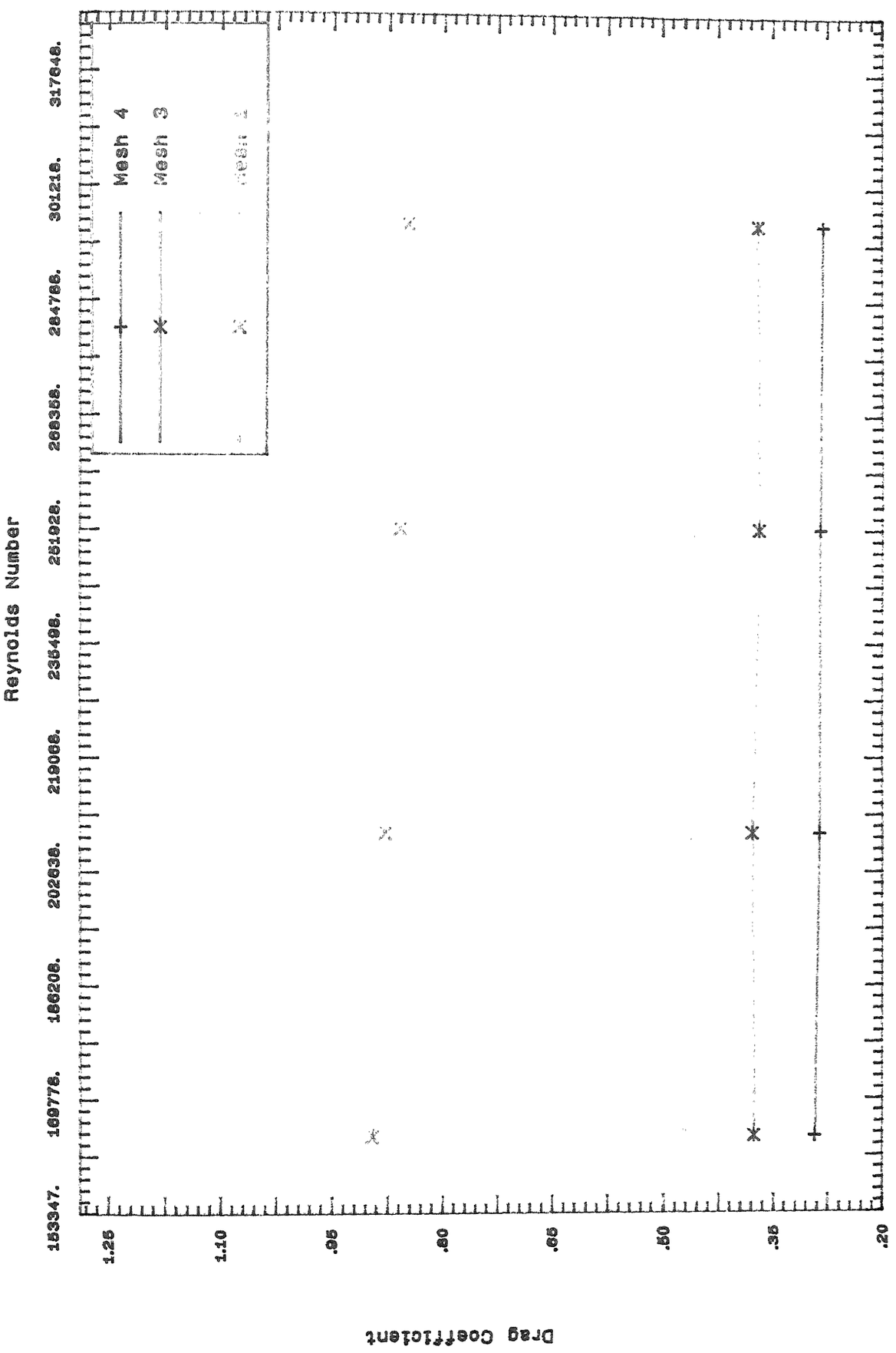

Fig 4 : Drag Coeff. for Included Cone Angle = 180 deg.

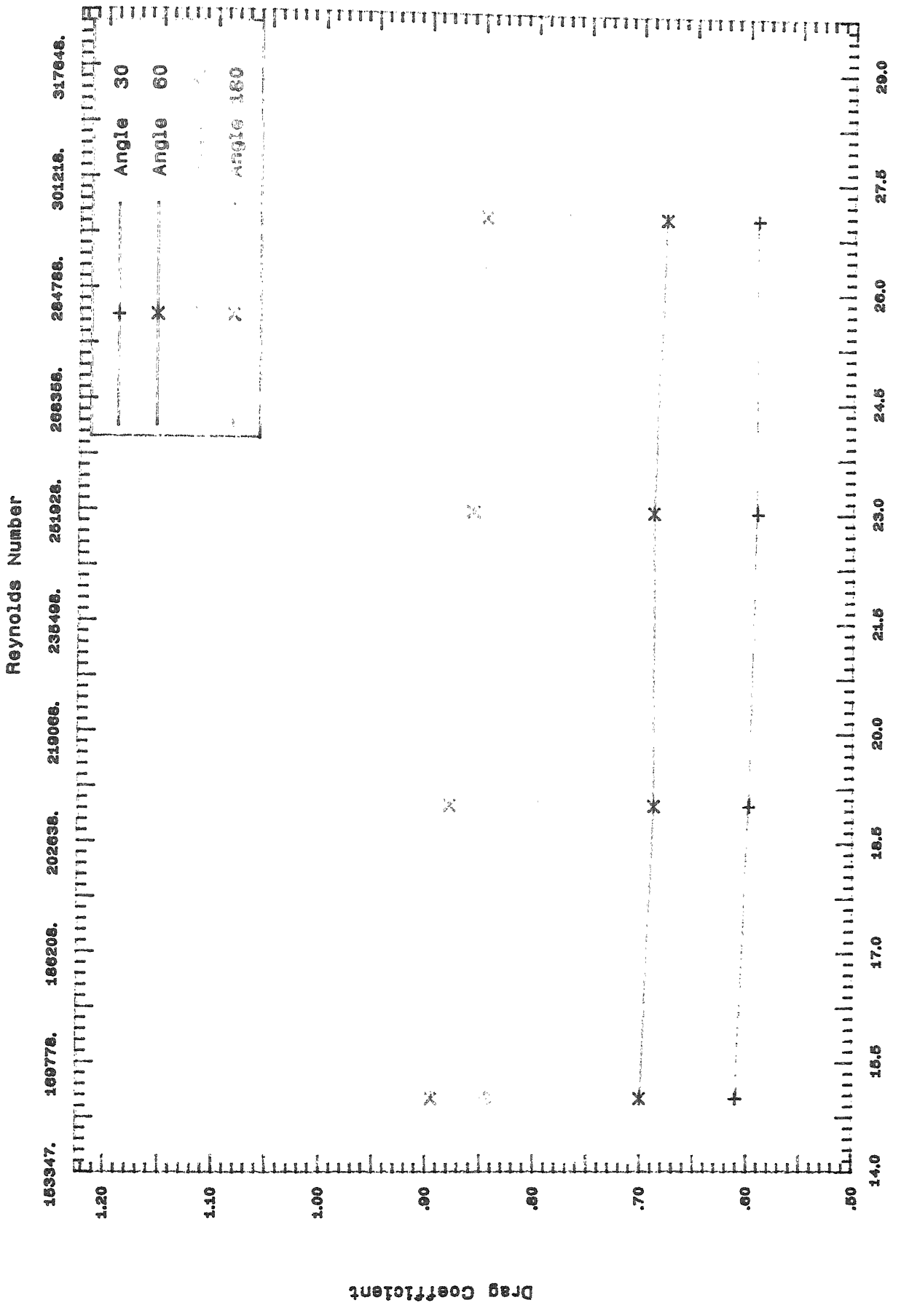

Fig 5 : Drag Coefficient for Mesh Type 1

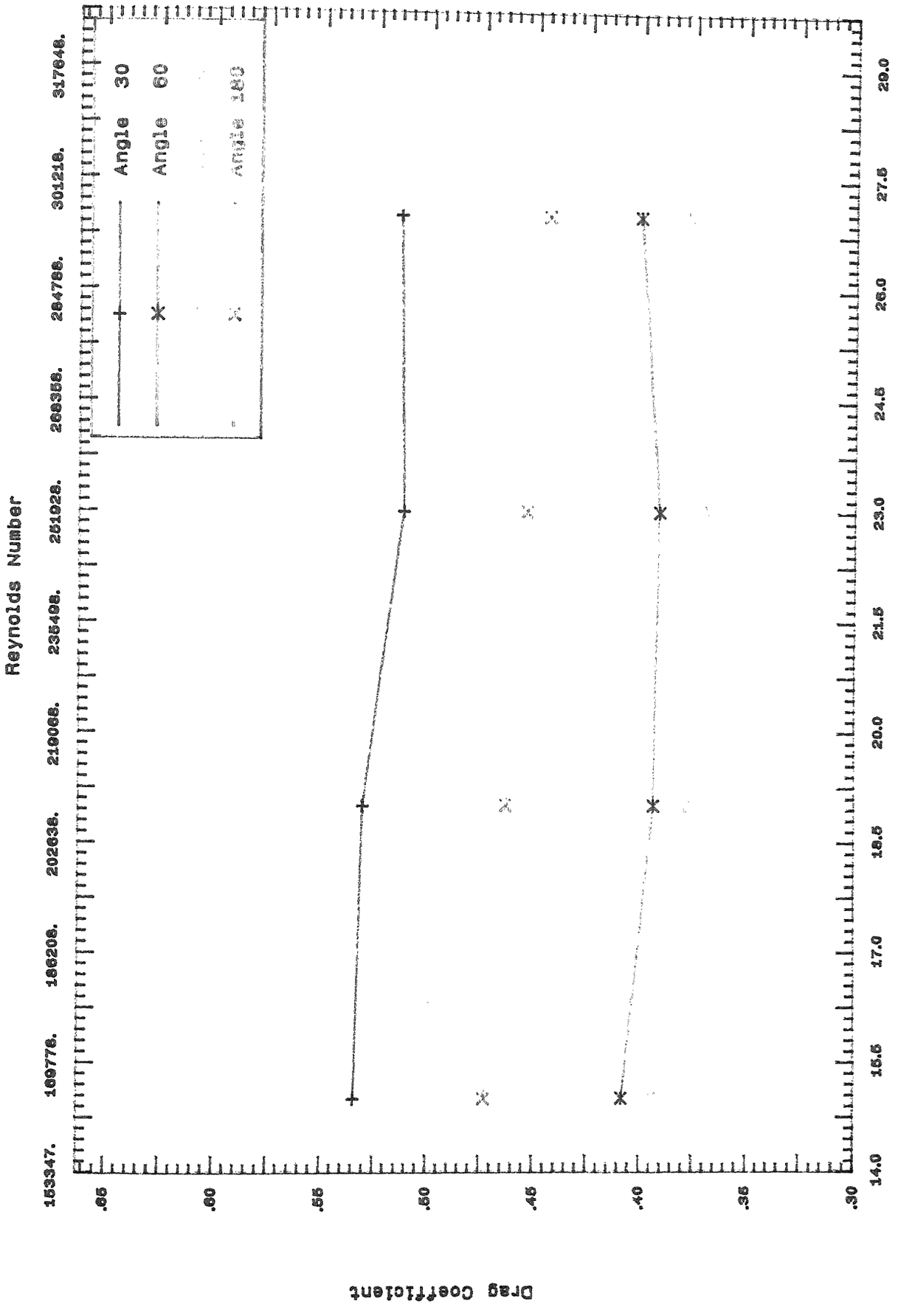

Fig 6 : Drag Coefficient for Mesh Type 2

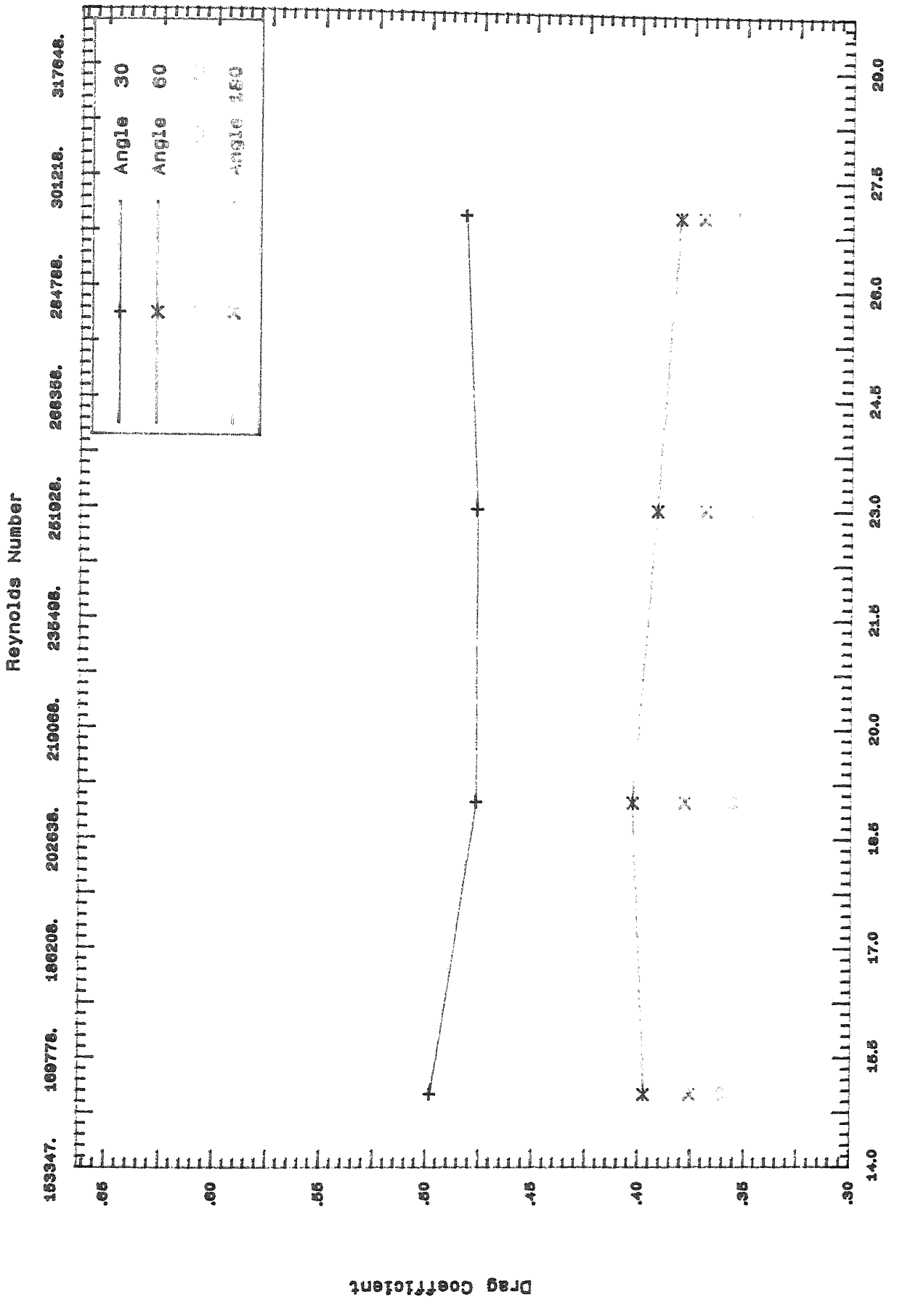

Fig 7 : Drag Coefficient for Mesh Type 3

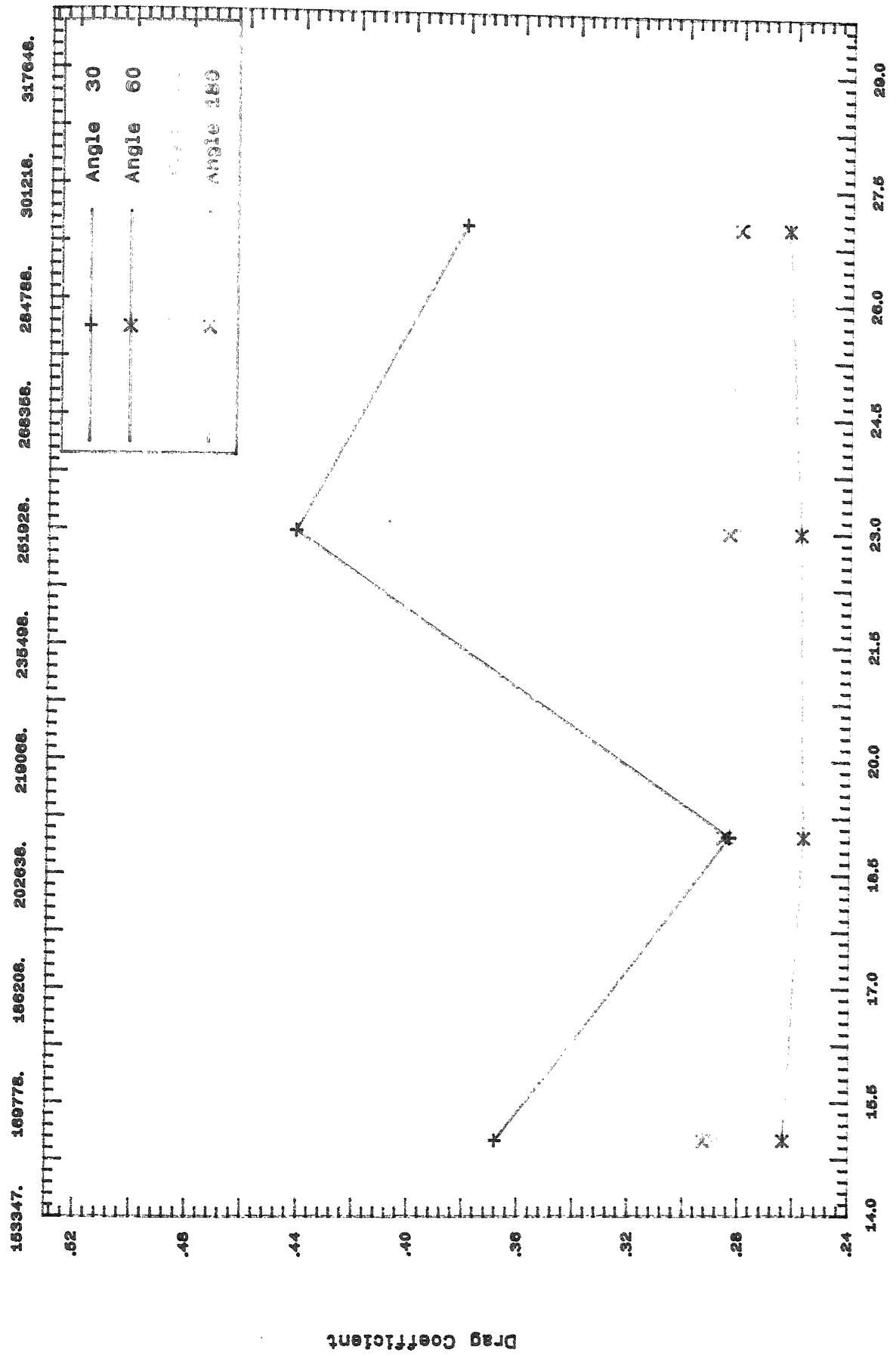

Fig 8 : Drag Coefficient for Mesh Type 4

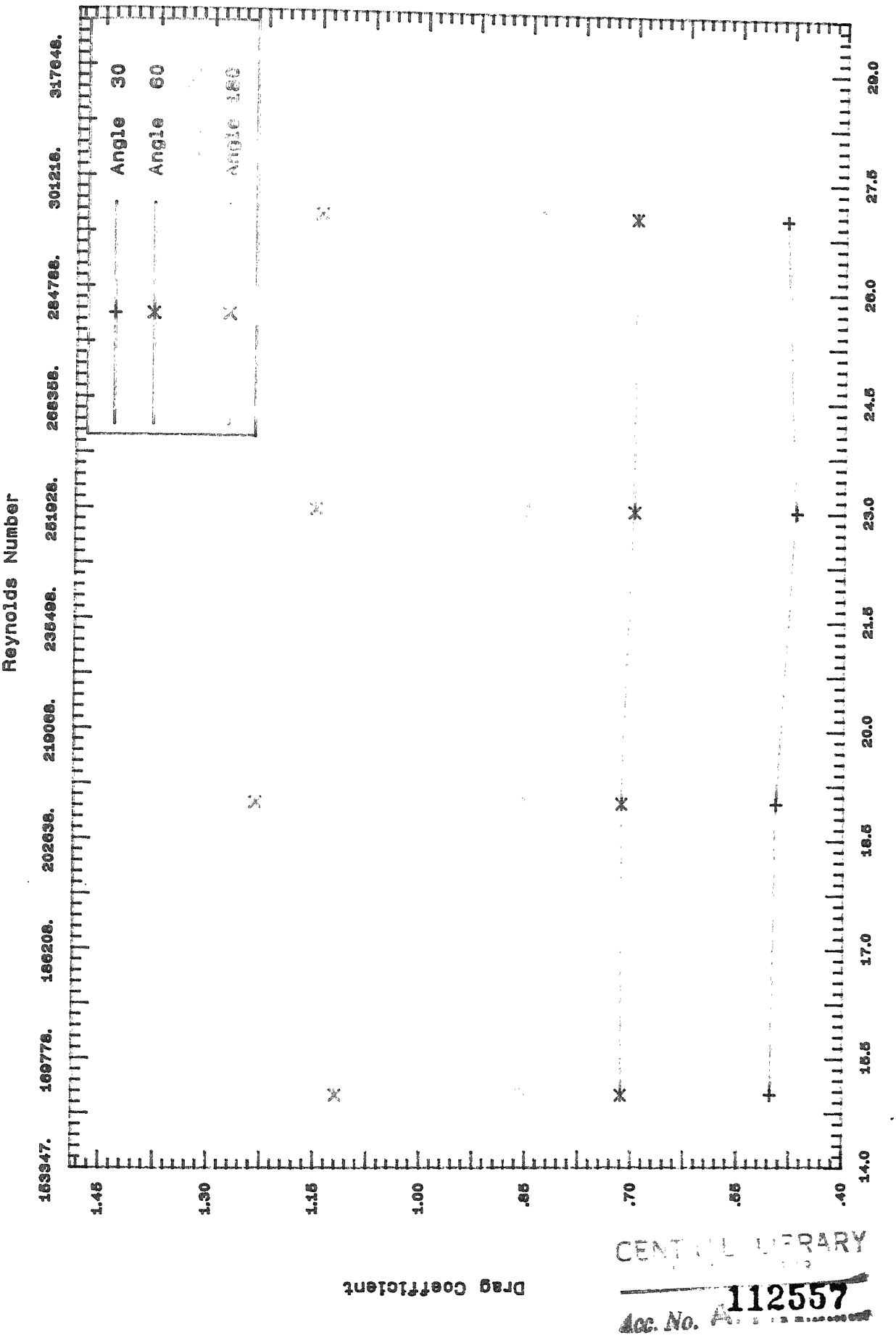

Fig 9 : Drag Coefficient for Solid Cone

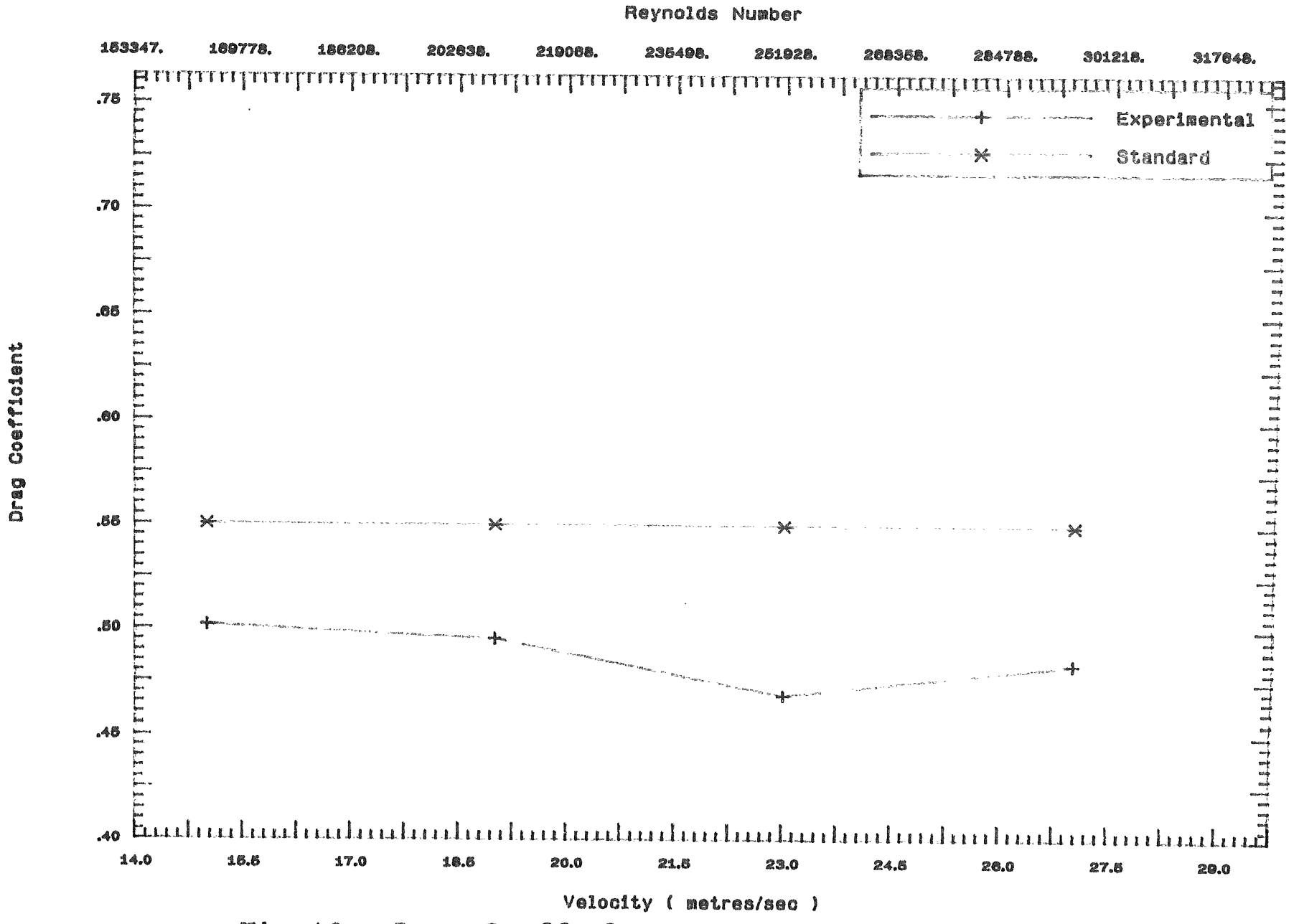

Fig 10 : Drag Coeff. for Solid Cone of Angle 30 deg.

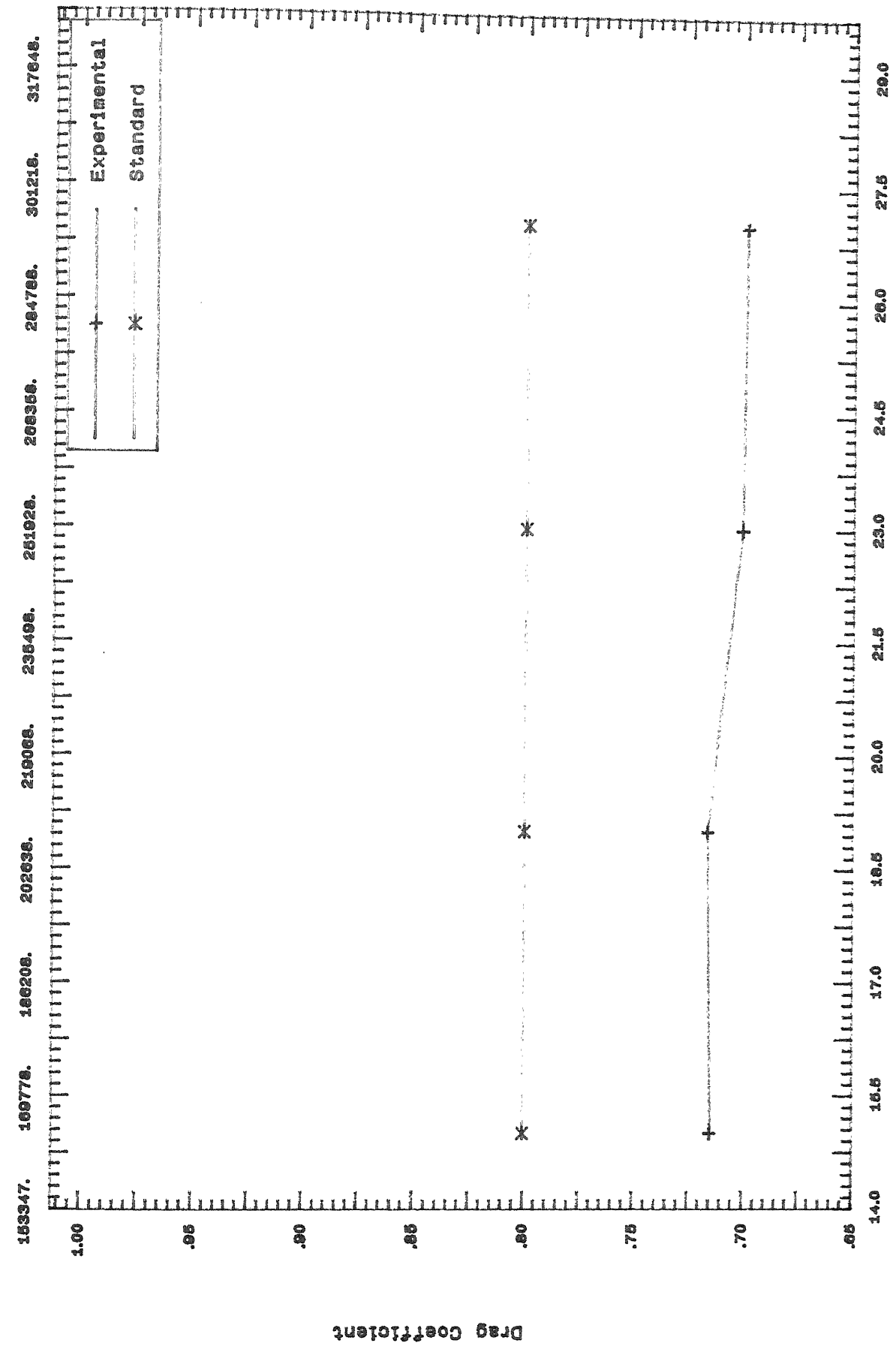

Fig 11 : Drag Coeff. for Solid Cone of Angle 60 deg.

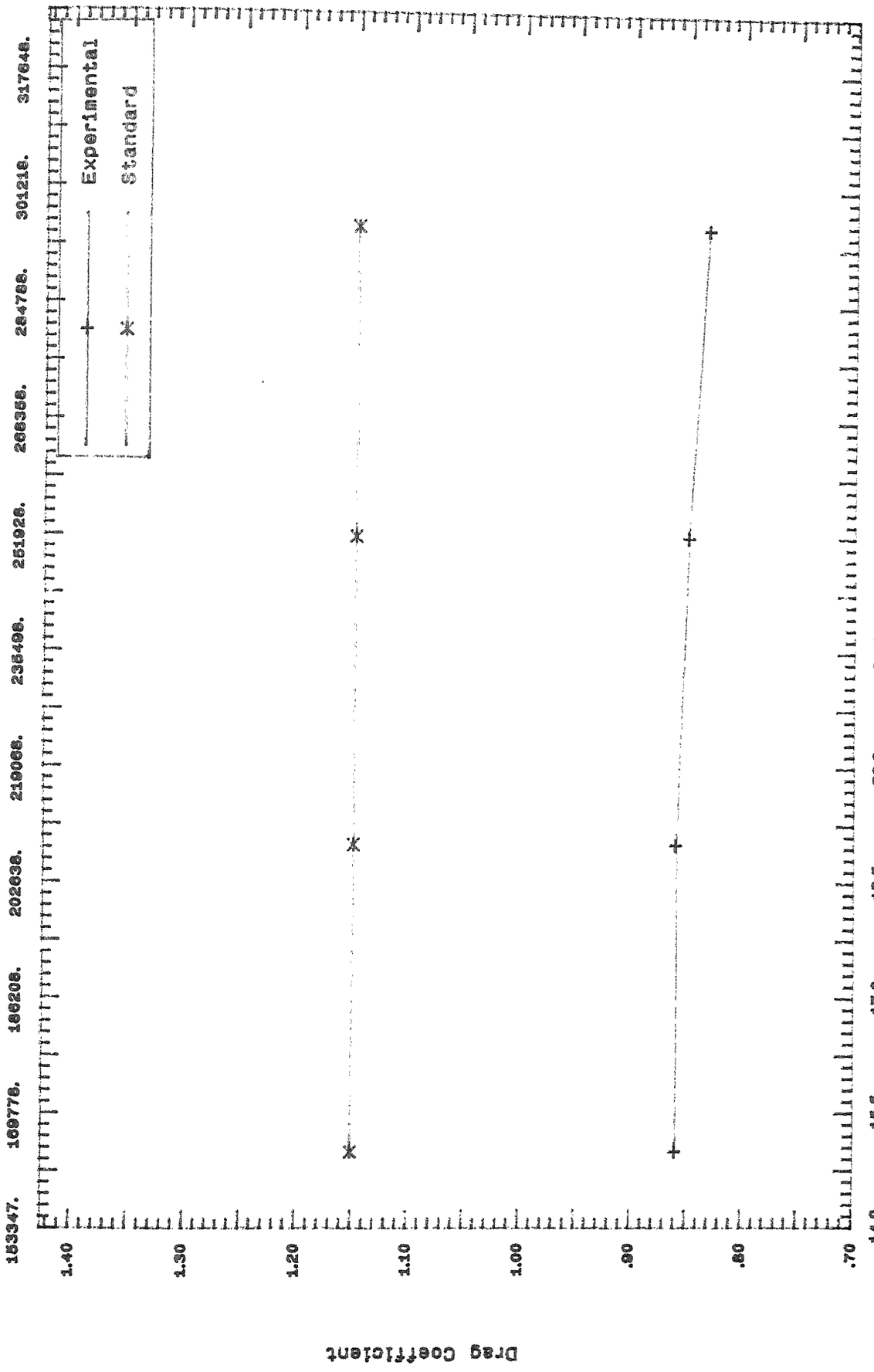

Fig 12 : Drag Coeff. for Solid Cone of Angle 90 deg.

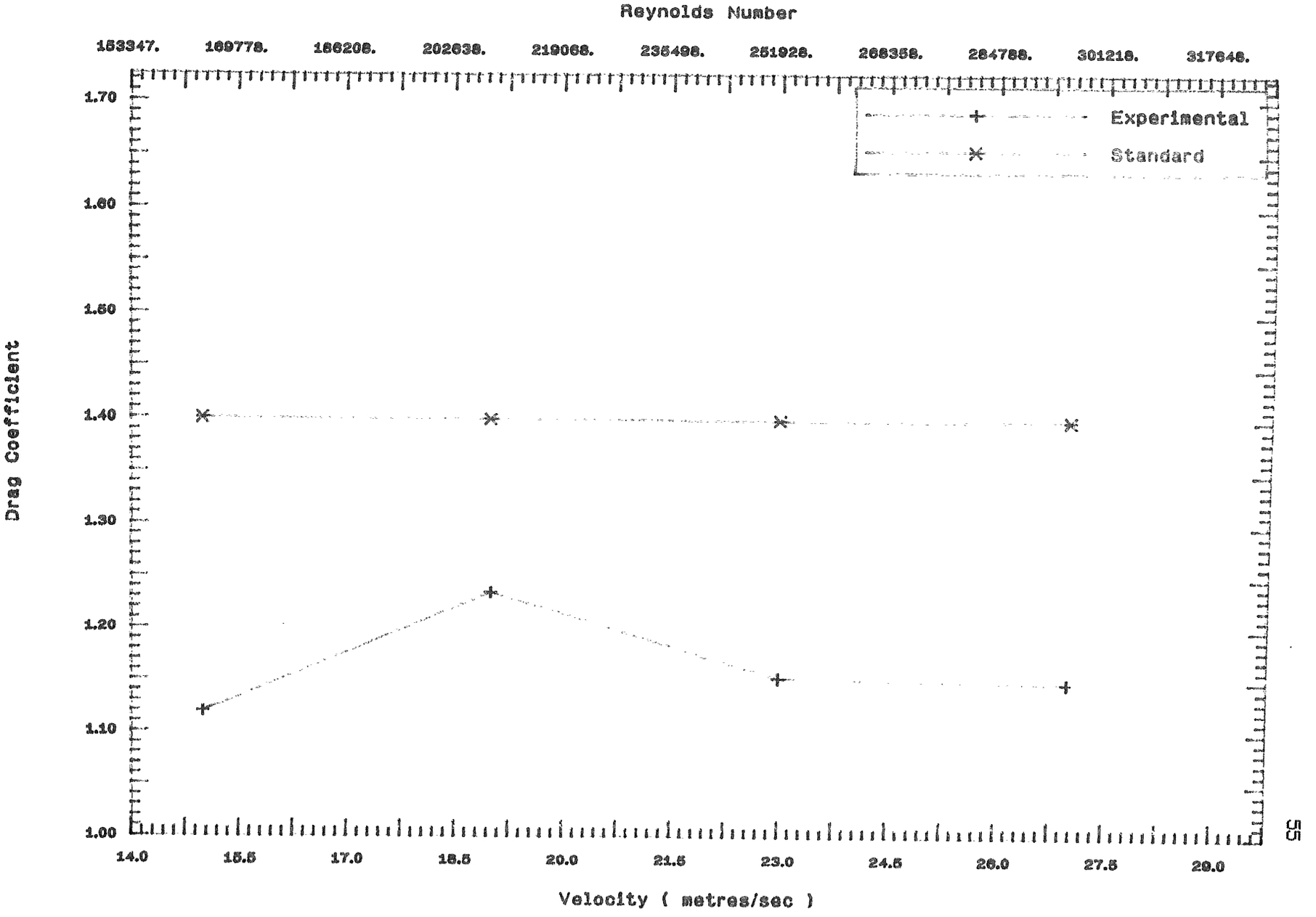

Fig 13 : Drag Coeff. for Solid Cone of Angle 180 deg.

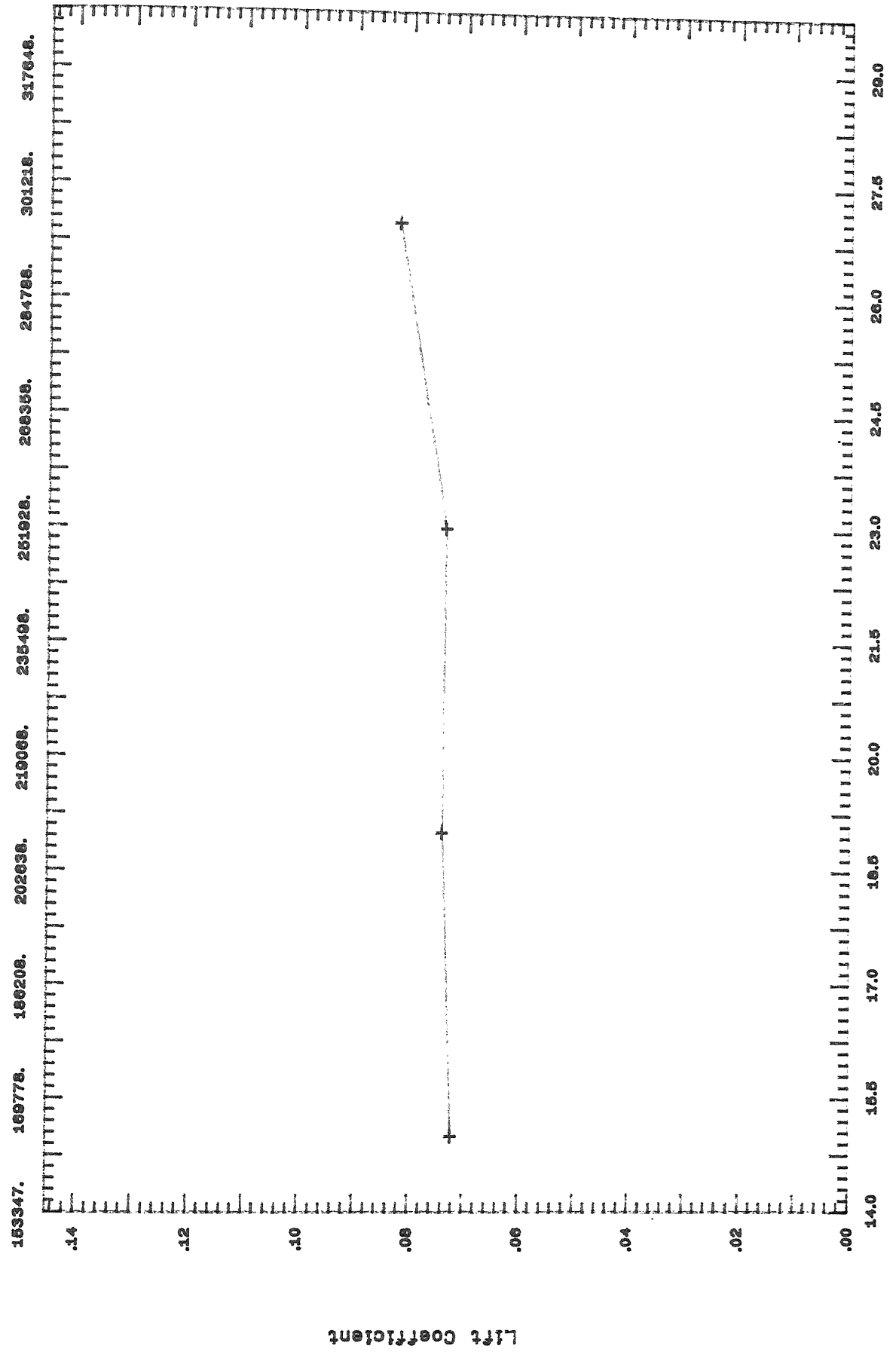

Fig 14 : Lift Coeff. for Perf. Cone of Mesh 1 and Angle 90 deg.

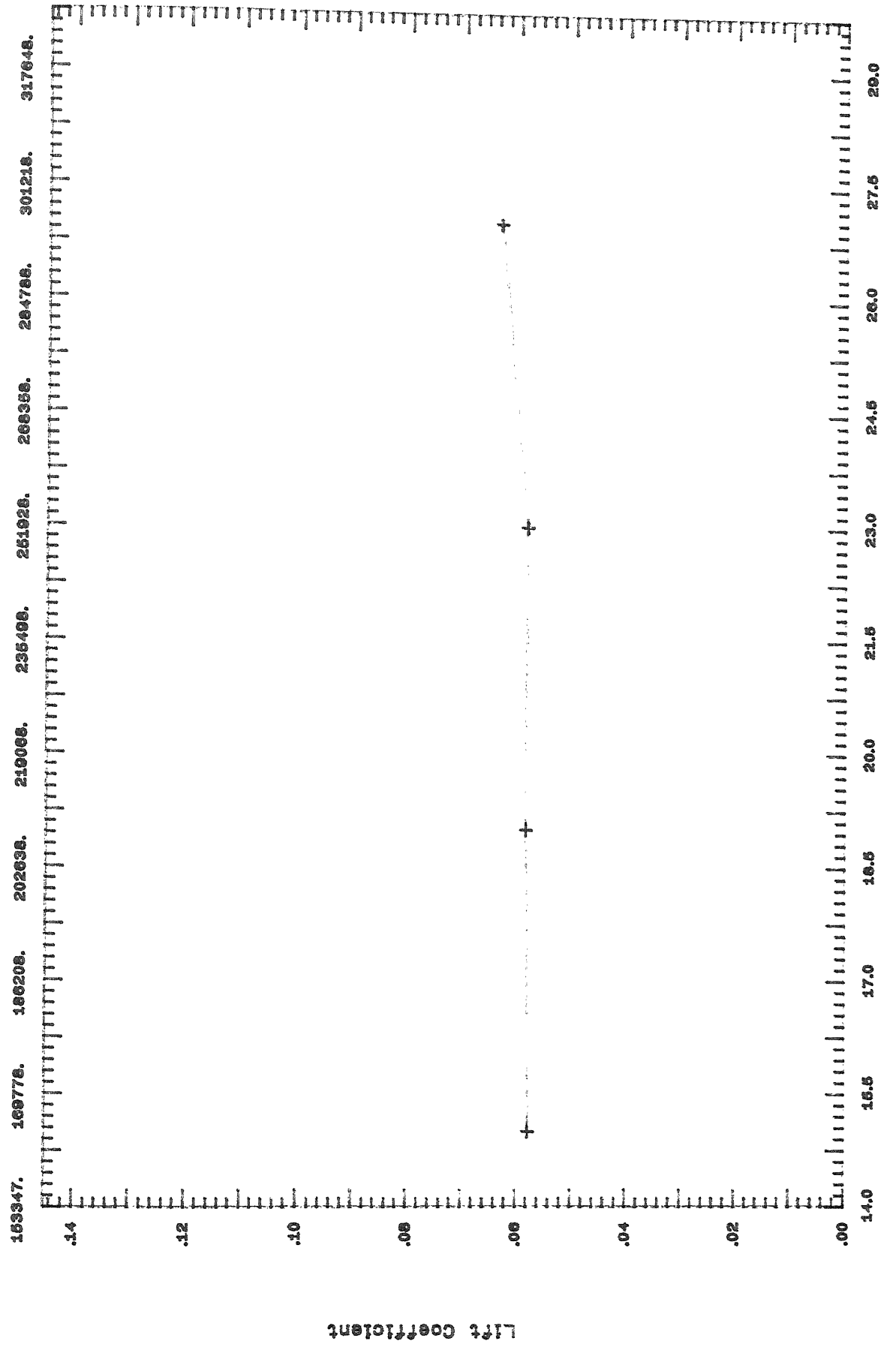

Fig 15 : Lift Coeff. for Perf. Cone of Mesh 4 and Angle 90 deg.

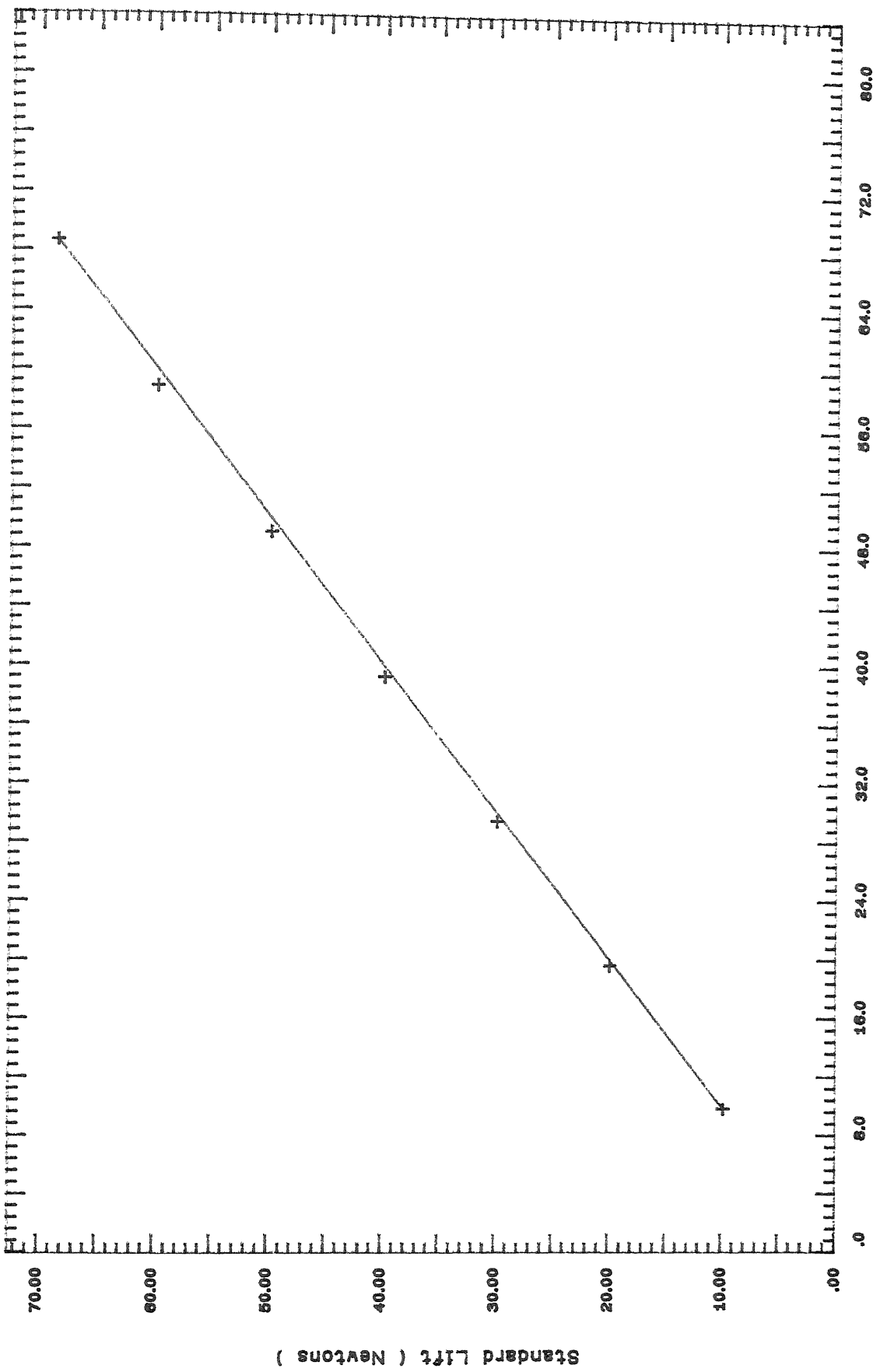

Fig 16 : Lift Calibration Curve

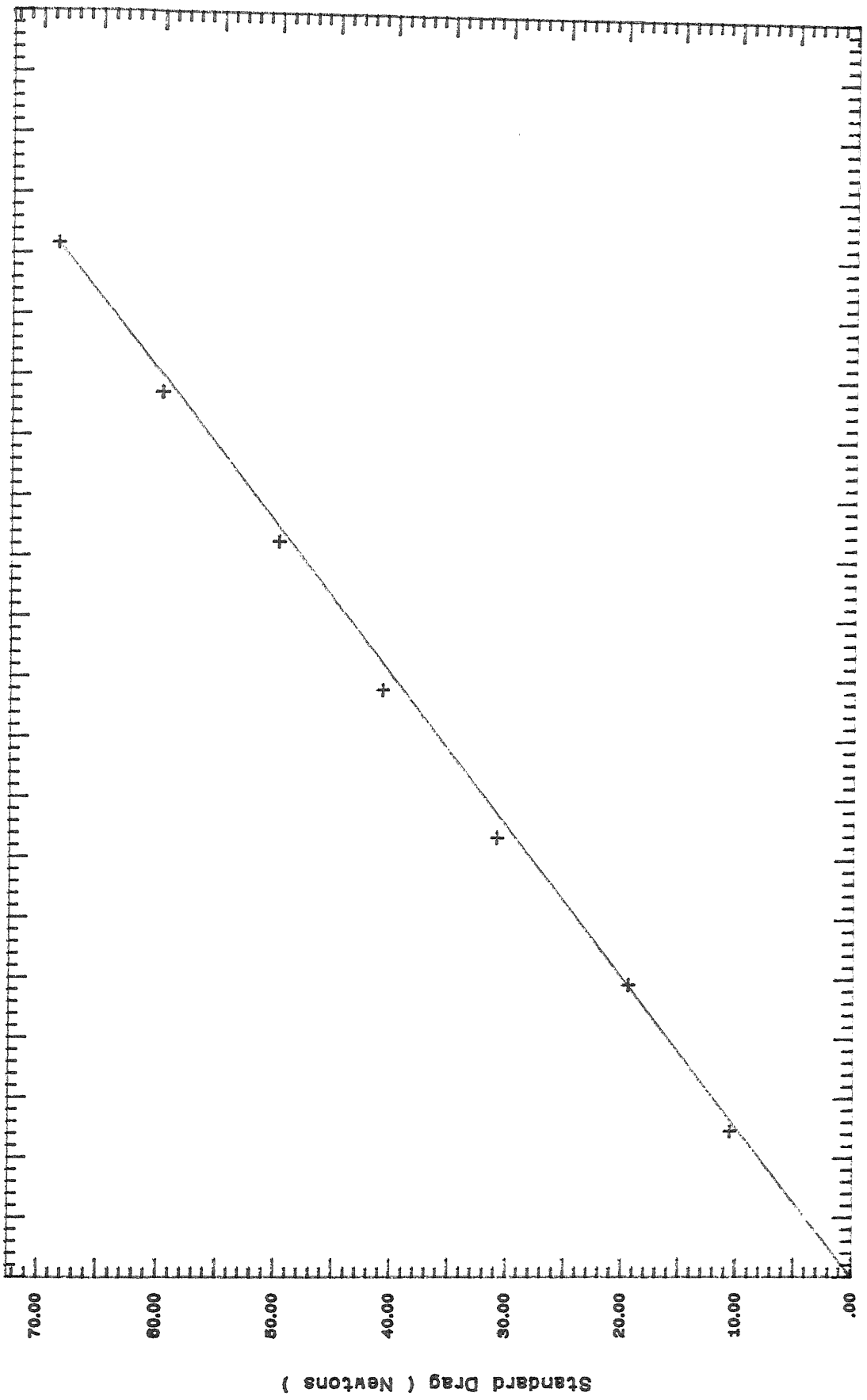

Fig 17 : Drag Calibration Curve

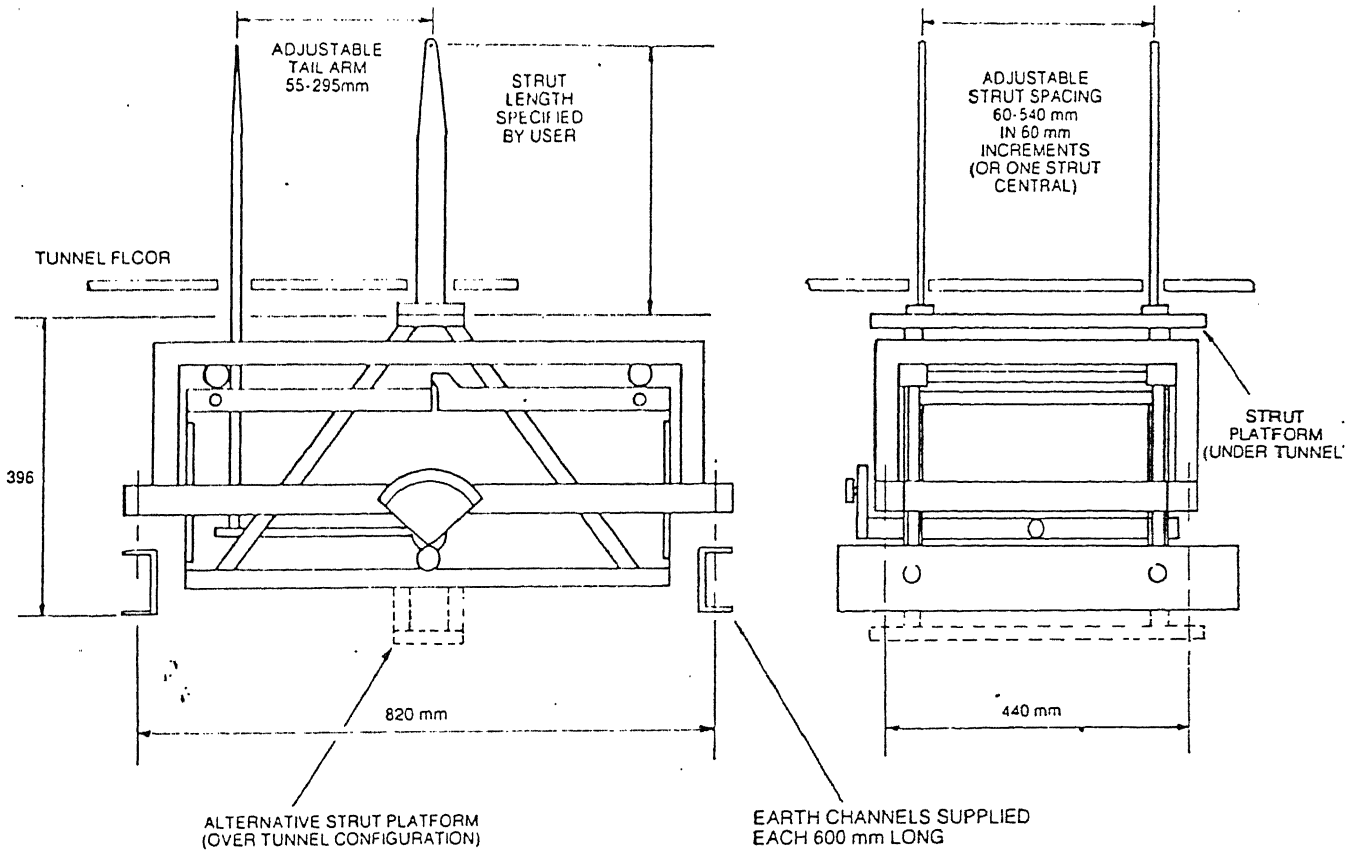

A SCHEMATIC VIEW OF THE BALANCE

FIG. 2

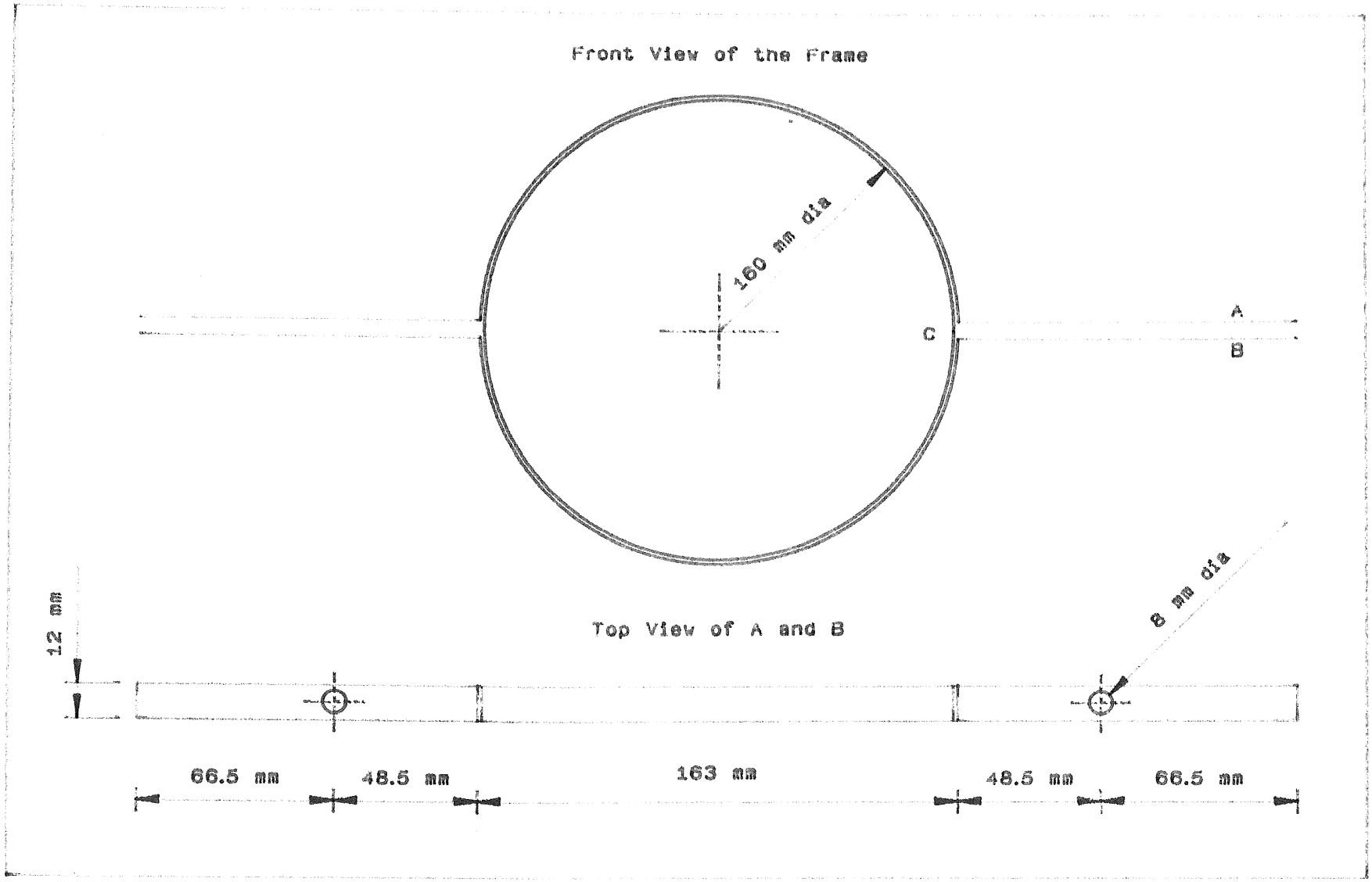

Fig 19 : Various Components of the frame

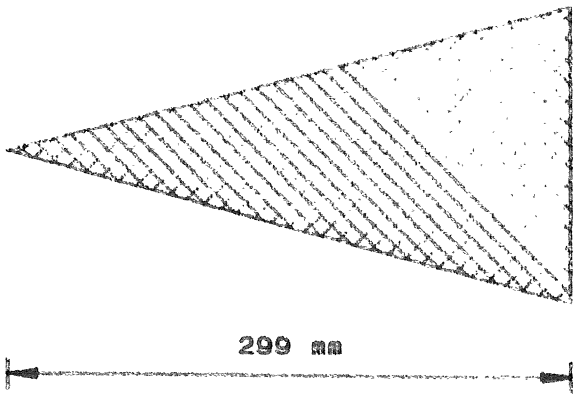

base dia = 160 mm , angle = 30 deg

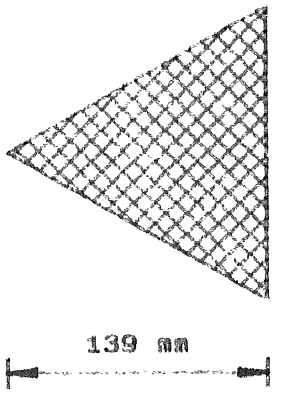

base dia = 160 mm , angle = 60 deg

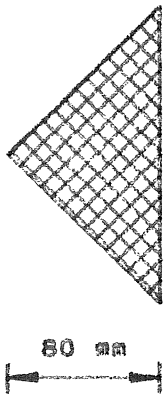

base dia = 160 mm , angle = 90 deg

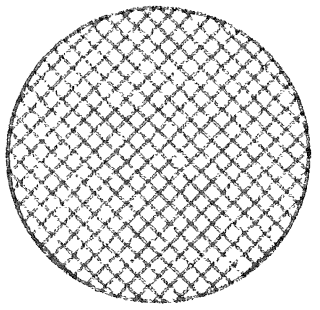

Length of cone = 0 mm

base dia = 160 mm , angle = 180 deg

Front View

Fig 20 : Sketch of the Conical Shell

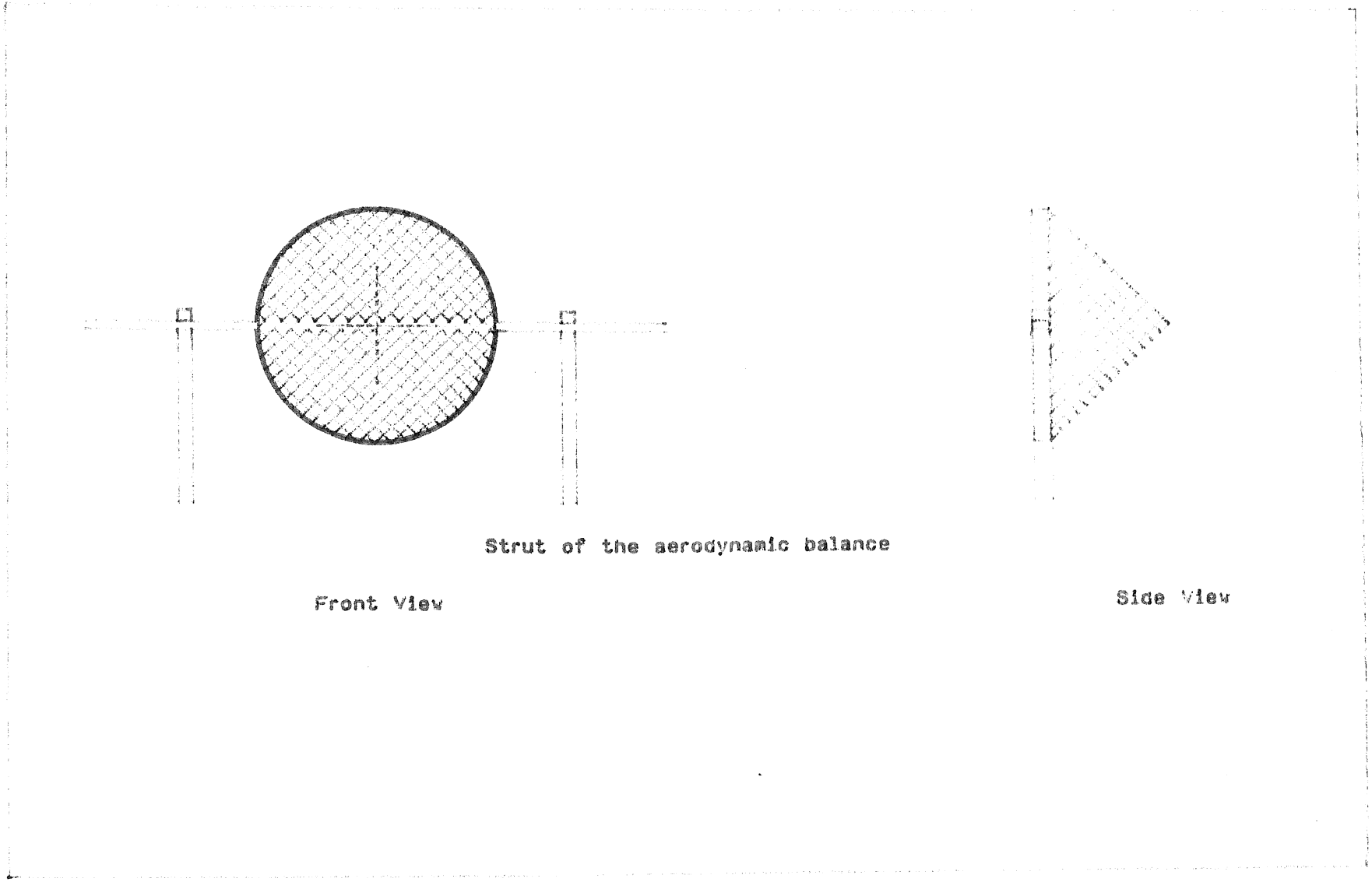

Fig 21 : Model as Mounted in the Wind Tunnel

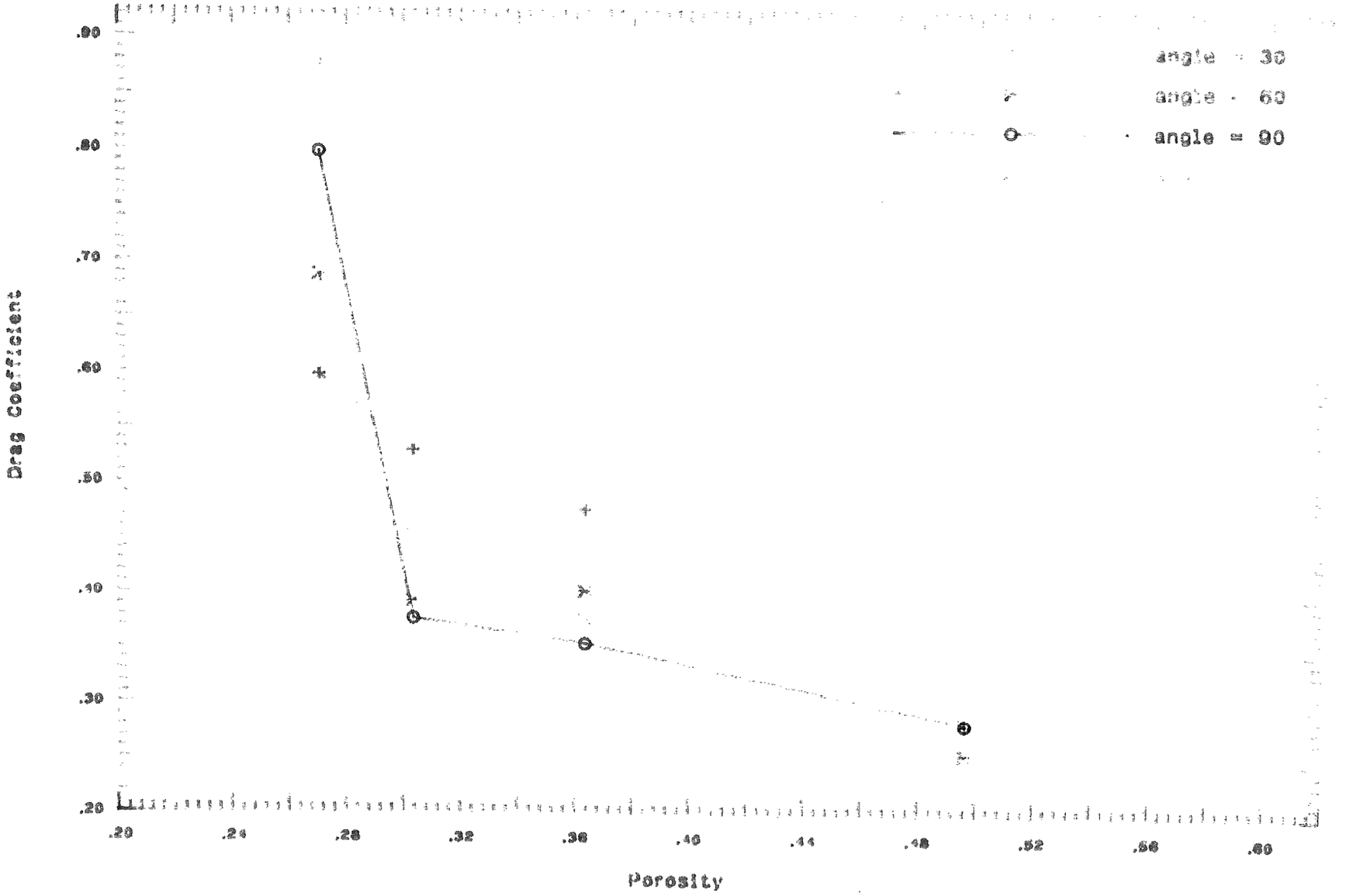

Fig 22 : Drag Coeff. for Velocity = 19 m/s

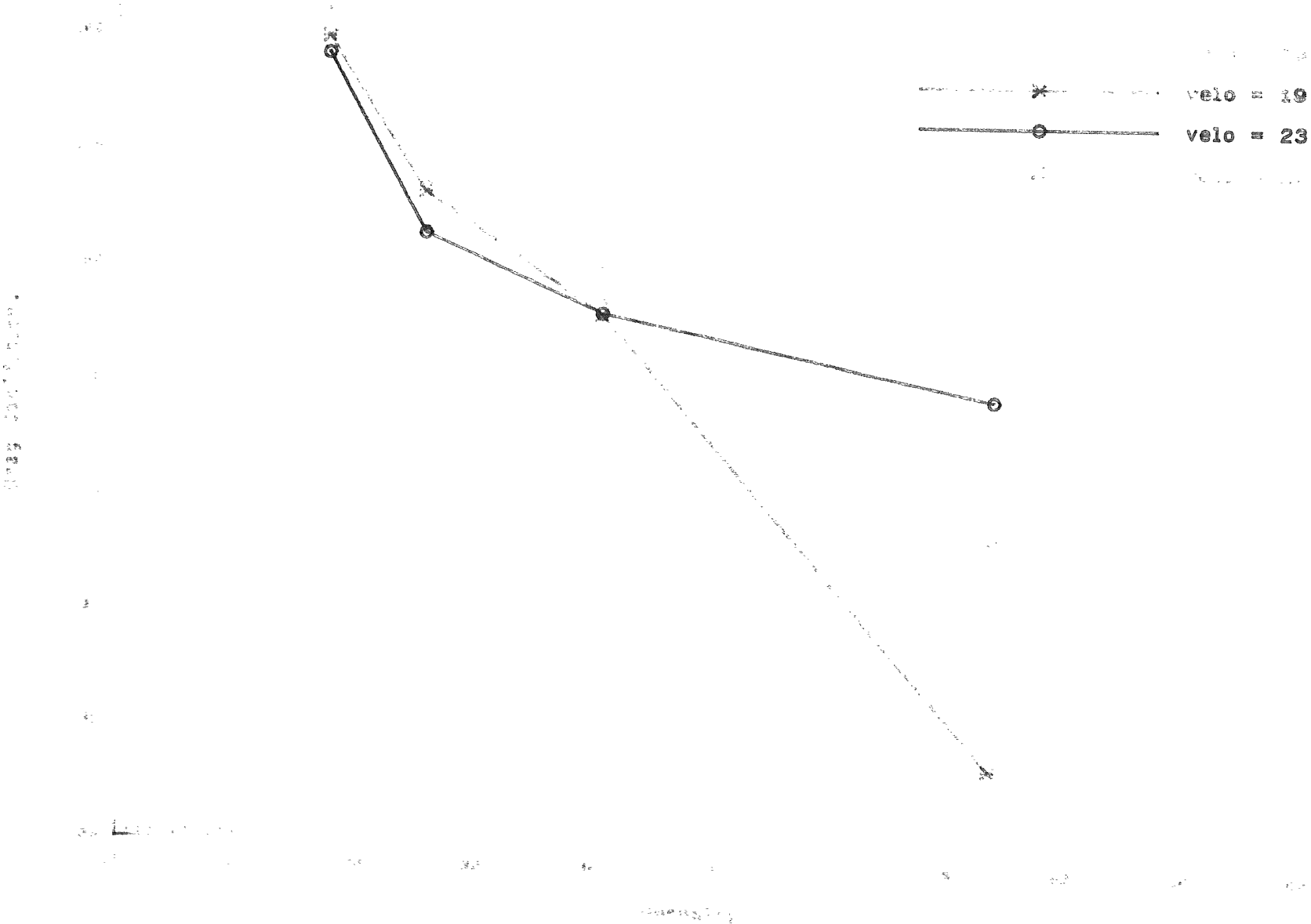

Fig 23 : [illegible]

APPENDIX 1

Conceptual Study of Bird hit Prevention Device

by

Dr. A. K. Gupta

In tropical and developing countries like India there are infrequent and yet consequential instances in which the birds, in particular vultures,flying near the airports are ingested into the turbojets engines during the take-off or landing phases of the aircraft flight. Such incidents have been encountered both by the civil and military aircrafts. The consequences of bird-hits have been the damage to the turbo-jet engine resulting in the loss of flight safety of the aircrafts and its occupants , financial losses due to repair or replacement of the damaged engine , and the flight delays due to rescheduling and/or re-routing of the airline's fleet of overworked aircrafts.

This conceptual study proposes the installation of a perforated conical shell ahead of the turbojet intake during the phases of take-off and landing to

act as a bird-hit prevention device operating from the ground level upto an altitude of about one kilometer . The perforated cone is formed in two halves and is retractable into the engine nacelles in a manner likely to be similar to the thrust reverser device installed in the tail region of the turbo-jet engine nacelle .

There are four aspects of the proposed bird-hit prevention device :

1) the aerodynamics of the perforated conical shell ,
2) the stuctural strength of the perforated conical shell to withstand the impact of bird-hit,
3) the retraction mechanism and its installation in the engine nacelle, and
4) the monitoring of the bird-hit prevention device .

The additional weight due to the device and its retraction and monitoring mechanism is not likely to be a design problem in view of the relatively heavy aircrafts with large payloads operating now in a routine manner .

The present paper will deal mainly with the

aerodynamic aspects of the perforated conical shells . Aerodynamic drag and the passage of the required amount of air flow , in particular during the take-off phase , are the important considerations .

The other parameters for a wind tunnel study of perforated conical shells are the cone angle , the ratio of the perforated frontal area to the cone frontal area , the ratio of the spacing between the cone base and the engine intake to the intake cone diameter , and the ratio of the suction pressure at the intake generated by the engine perforated cone base pressure .

A wind tunnel study is in progress where the aerodynamics of the perforated conical shells with respect to the cone angle and the perforated area is being investigated . The results of this experimental investigation will be presented .

APPENDIX 2

Experimental Results

True drag of the perforated conical shells (Newtons)					
Mesh Type and angle		Velocity			
		15 m/s	19 m/s	23 m/s	27 m/s
Mesh 1	30°	1.69	2.66	3.85	5.31
	60°	1.94	3.06	4.49	6.09
	90°	2.34	3.55	4.95	6.93
	180°	2.48	3.91	5.60	7.62
Mesh 2	30°	1.48	2.36	3.34	4.62
	60°	1.13	1.82	2.60	3.59
	90°	1.09	1.68	2.41	3.40
	180°	1.31	2.06	2.96	3.99
Mesh 3	30°	1.38	2.12	3.11	4.34
	60°	1.10	1.79	2.55	3.44
	90°	1.00	1.58	2.25	3.17
	180°	1.04	1.68	2.40	3.32
Mesh 4	30°	1.02	1.26	2.88	3.42
	60°	0.73	1.14	1.68	2.36
	90°	0.80	1.26	1.83	2.50
	180°	0.81	1.27	1.85	2.52